HMGN2 represses gene transcription *via* interaction with transcription factors Lef-1 and Pitx2 during amelogenesis

Steven Eliason[1], Dan Su[1], Flavia Pinho[2], Zhao Sun[3], Zichao Zhang[4], Xiao Li[5], Mason Sweat[6], Shankar R. Venugopalan[7], Bing He[8], Michael Bustin[8], and Brad A. Amendt[1,7,*]

From the [1]Department of Anatomy and Cell Biology and the Craniofacial Anomalies Research Center, Carver College of Medicine, The University of Iowa, Iowa City, Iowa, USA; [2]Janssen R&D, LLC, San Diego, California, USA; [3]Washington University St Louis, St Louis, Missouri, USA; [4]Institute for Biosciences and Technology, Houston, Texas, USA; [5]Texas Heart Institute, Houston, Texas, USA; [6]Boston Children's Hospital, Harvard Medical School, Boston, Massachusetts, USA; [7]Department of Orthodontics, The University of Iowa, Iowa City, Iowa, USA; [8]Protein Section, Laboratory of Metabolism, Center for Cancer Research, National Cancer Institute, National Institutes of Health, Bethesda, Maryland, USA

Edited by Ronald Wek

The chromatin-associated high mobility group protein N2 (HMGN2) cofactor regulates transcription factor activity through both chromatin and protein interactions. *Hmgn2* expression is known to be developmentally regulated, but the post-transcriptional mechanisms that regulate *Hmgn2* expression and its precise roles in tooth development remain unclear. Here, we demonstrate that HMGN2 inhibits the activity of multiple transcription factors as a general mechanism to regulate early development. Bimolecular fluorescence complementation, pull-down, and coimmunoprecipitation assays show that HMGN2 interacts with the transcription factor Lef-1 through its HMG-box domain as well as with other early development transcription factors, Dlx2, FoxJ1, and Pitx2. Furthermore, EMSAs demonstrate that HMGN2 binding to Lef-1 inhibits its DNA-binding activity. We found that Pitx2 and Hmgn2 associate with H4K5ac and H3K4me2 chromatin marks in the proximal *Dlx2* promoter, demonstrating Hmgn2 association with open chromatin. In addition, we demonstrate that microRNAs (miRs) *mir-23a* and *miR-23b* directly target *Hmgn2*, promoting transcriptional activation at several gene promoters, including the *amelogenin* promoter. *In vivo*, we found that decreased *Hmgn2* expression correlates with increased *miR-23* expression in craniofacial tissues as the murine embryo develops. Finally, we show that ablation of *Hmgn2* in mice results in increased *amelogenin* expression because of increased Pitx2, Dlx2, Lef-1, and FoxJ1 transcriptional activity. Taken together, our results demonstrate both post-transcriptional regulation of *Hmgn2* by *miR-23a/b* and post-translational regulation of gene expression by Hmgn2–transcription factor interactions. We conclude that HMGN2 regulates tooth development through its interaction with multiple transcription factors.

High mobility group N (HMGN) is a family of nonhistone chromatin architectural proteins that bind to the nucleosome core structure independent of DNA sequence to affect chromatin structure and function and regulate transcription (1–6). These nucleosome-binding proteins can colocalize with epigenetic marks of active chromatin and cell type–specific enhancers/promoters and regulate transcription levels (4–7). Hmgn2 may be required for stem cell maintenance through specific activation of stem cell factors and induction of active epigenetic marks (3, 5, 8, 9). We have previously shown that Hmgn2 forms an inactive transcriptional complex with transcription factor Pitx2, which bound to chromatin, and poised to activate transcription (10). This inactive complex is then activated through Wnt signaling and the interaction with β-catenin (β-cat) (10). A similar mechanism was proposed recently stating that HMGN proteins open chromatin structure at enhancer regions maintaining them in a poised open chromatin state, ready for rapid stimuli-dependent gene expression (4). More recently, a study demonstrated that HMGN2 protein could localize to cell-specific enhancers to modulate the chromatin epigenetic landscape (5). These data all point to HMGN2 as a critical regulator of transcriptional activation of gene expression. *Hmgn2* expression occurs during early mouse embryogenesis and affects the timing of early embryonic development in the mouse (11). The expression of *Hmgn2* is reduced in adult tissues (12), and in multiple tissues, it correlates with gene expression regulating developmental processes.

Lymphoid enhancer–binding factor 1 gene (*Lef-1*) plays a critical role in organ, craniofacial, and tooth development. The Lef-1 protein contains an HMG-box domain and has been shown to act as a transcription factor (13). The role of *Hmgn2* in development remains unclear and, in this report, we analyzed *Hmgn2*-null mice for developmental defects and its interaction with Lef-1.

Pitx2 is the earliest transcription factor observed in tooth development, which marks dental epithelial but not mesenchymal tissues and directly activates several genes regulating dental epithelial stem cells, embryonic tooth development, and enamel formation (14–19). *Pitx2* has long been considered as a master regulator of the transcriptional hierarchy in early tooth development, including stem cells (20, 21). Pitx2 regulates

* For correspondence: Brad A. Amendt, brad-amendt@uiowa.edu.

HMGN2 activity during development

Sox2 and *Lef-1* expression in the dental epithelium, and we previously demonstrated that HMGN2 represses *Pitx2* and *Sox2* transcriptional activation (10, 22–25). The ablation of *Lef-1* in the dental epithelium leads to severe tooth developmental defects, causing an arrest during the transition from bud to cap stage (26, 27). We have shown that conditional overexpression of *Lef-1* in the dental epithelium results in a new stem cell compartment with increased dental epithelial cell proliferation affecting amelogenin expression and enamel formation (24).

MicroRNA (miR)-mediated gene silencing plays important roles in many biological processes, such as cell proliferation, differentiation, and death (28, 29). miRs are ∼22 nt endogenous RNAs that bind to sequences within $3'UTR$ of protein-coding genes to post-transcriptionally regulate gene function (30). miRs have been reported to play critical roles in tooth development. For example, the inactivation of *Dicer1* in dental epithelium results in severe phenotypes, such as loss of enamel and multiple teeth (31). *miR-23a* and *miR-23b* are encoded by the *miR-23a-27a-24* (mouse chromosome 8) and *miR-23b-27b-24* clusters (mouse chromosome 13), respectively, and their expression has been reported to play an important role in endocrine homeostasis (32), cell death (33), glutamine metabolism (34), and cancer development (35). A large-scale screen for miR expression profiles in the tooth germs of miniature pigs reveals that both *miR-23a and b* are highly expressed during tooth development (36). We showed that *miR-23a+b* are highly expressed in the mouse dental epithelial cells using microarray analysis by comparing the miR expression profiles between differentiated and undifferentiated dental epithelial tissues (31).

In this report, we describe new molecular and developmental mechanisms for the HMGN2 protein. HMGN2 is a chromatin-associated factor able to inhibit transcription factor DNA binding and transcriptional activation. Furthermore, HMGN2 acts as a general regulator of multiple transcription factors and is directly targeted by *miR-23a+b*. Interestingly, as development progresses the expression of *Hmgn2* in the mouse gradually decreases in a manner that was inversely correlated with *miR-23a+b* during tooth development and *amelogenin* expression, the gene required for enamel formation. Finally, deletion of *Hmgn2* in mice resulted in increased *amelogenin* expression affecting tooth development. Our research defines HMGN2 as a general regulator of transcription factor activity through protein interactions associated with active chromatin marks. This report describes both post-transcriptional and post-translational mechanisms to regulate multiple genes by HMGN2.

Results

HMGN2 interacts with Lef-1 in the nucleus and represses Lef-1 transcriptional activity

We have used a cell model to demonstrate a direct interaction between Lef-1 and HMGN2 and their cellular localization by performing the bimolecular fluorescenc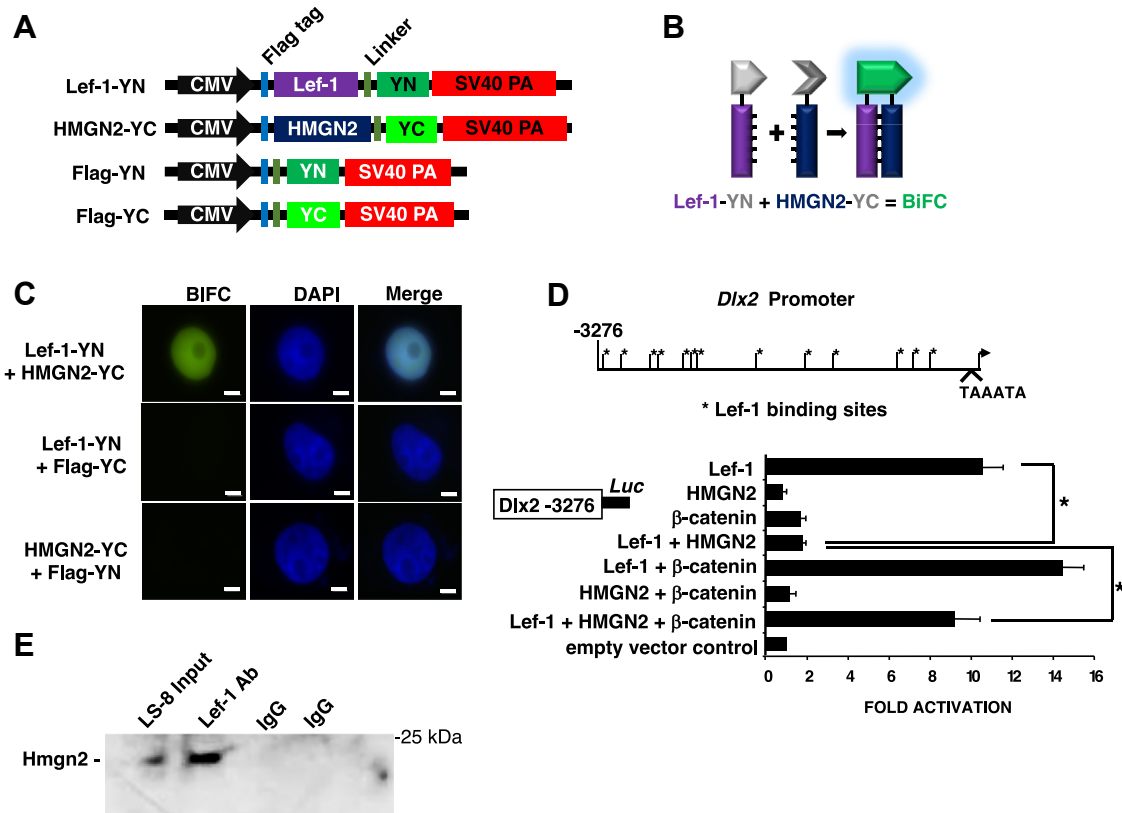e complementation (BiFC) assay. *Lef-1* was ligated to the N terminus of an *EYFP-N* (EYFP [enhanced YFP]) coding sequence, and *HMGN2* was cloned to the N-terminal region of an *EYFP-C* sequence (Fig. 1A). Direct physical association between Lef-1-YN and HMGN2-YC resulted in fluorescence under EYFP excitation wavelength because of interactions between N and C fragments of the EYFP protein (Fig. 1B) (37, 38). As shown in Figure 1C, Lef-1-YN and HMGN2-YC interact to produce fluorescence that is confined to the nucleus. As controls, transfecting either Lef-1-YN with the FLAG-EYFP-C fragment (FLAG-YC) or HMGN2-YC with FLAG-EYFP-N fragment (FLAG-YN) did not emit fluorescence (Fig. 1C). These results indicate that Lef-1 and HMGN2 interact in the nucleus of living cells.

We have demonstrated that HMGN2 interacts with Pitx2 and Sox2 to form an inactive complex to inhibit Pitx2 and Sox2 DNA-binding activity (23–25, 39). Dlx2 is required for craniofacial and tooth development, and we have shown that Pitx2 and Lef-1 regulate the *Dlx2* promoter (23, 40, 41). To determine if HMGN2 regulates Lef-1 activation of the *Dlx2* promoter, we cotransfected the *Dlx2* promoter luciferase reporter, Lef-1 and ß-catenin with/without HMGN2 in LS-8 oral epithelial cells. The luciferase results show that Lef-1 activated the *Dlx2* promoter, but this activation was significantly reduced while overexpressing HMGN2 (Fig. 1D). Furthermore, cotransfection with β-cat rescued Lef-1 transcriptional inhibition by the HMGN2 protein. Therefore, HMGN2 inhibits Lef-1 transactivation of the *Dlx2* promoter, and the Lef-1 interaction with β-cat overcomes this inhibition. Coimmunoprecipitation (co-IP) assays also demonstrate a direct interaction of endogenous Hmgn2 with endogenous Lef-1 in LS-8 oral epithelial cells (Fig. 1E).

HMGN2 interacts with the Lef-1 HMG-box domain

To map the Lef-1 domain that interacts with HMGN2, glutathione-*S*-transferase (GST) pull-down experiments were performed using purified bacteria-expressed proteins. A schematic diagram of the immobilized GST-Lef-1 full-length and truncated proteins is shown (Fig. 2A). Full-length HMGN2 protein was used in the pull-down experiments and immobilized GST-Lef-1, GST-Lef-1 ΔN113, GST-Lef-1ΔN295, and GST-Lef-1 ΔN113-ΔC34 all bound HMGN2 protein (Fig. 2B). However, GST-Lef-1 ΔN363 and GST-Lef-1 ΔN113-ΔC102 did not bind HMGN2 protein (Fig. 2B). From these experiments, we identified that HMGN2 interacts with the Lef-1 HMG-box domain (Fig. 2A).

Because it is well known that β-cat and Lef-1 interact, we asked if Lef-1 interacts with HMGN2 in the presence of β-cat. An immunoprecipitation (IP) assay was performed to detect HMGN2 binding to endogenous β-cat and transfected Lef-1 and HMGN2 in Chinese hamster ovary (CHO) cells (Fig. 2C). β-cat was immunoprecipitated from CHO cells transfected with plasmids for HMGN2 and Lef-1, and immunoprecipitates were then probed for HMGN2 protein. HMGN2 bound only to the β-cat–Lef-1 complex and not to β-cat alone (Fig. 2C).

Figure 1. Lef-1 interacts with HMGN2 in the nucleus, and HMGN2 represses Lef-1 transcriptional activity. *A* and *B*, schematic of the constructs used in bimolecular fluorescence complementation (BiFC) assay. *Lef-1* (murine clone) was cloned into the pFLAG-CMV-2 plasmid (Sigma) containing an N-terminal fragment of EYFP, and *HMGN2* (human clone) FC was ligated to a C-terminal fragment of EYFP in the pFLAG-CMV-2 plasmid. YN or YC fragments only were ligated into the vector and used as negative controls. The interaction between the proteins facilitates the association of YN and YC fragments to produce fluorescence under EYFP excitation wavelength. *C*, the constructs were transfected into HEK-293 cells. After 24 h, Nikon 80i fluorescence microscope was used to detect the fluorescence. The scale bar represents 5 μm. *D*, HMGN2 represses Lef-1 transcriptional activation. A schematic of the 3276 bp *Dlx2* promoter is shown with Lef-1–binding sites. LS-8 cells were transfected with *Dlx2* promoter luciferase reporter gene (5 μg) and *Lef-1* and/or β-catenin with/without *HMGN2* expression plasmids (2.5 μg) and a β-galactosidase expression construct (0.5 μg). After 48 h, luciferase and β-galactosidase activities were measured. The luciferase activities were shown as mean fold activation compared with the normalized luciferase activity in empty vector (pcDNA 3.1) with *Dlx2* promoter reporter. N = 4, *$p < 0.05$. *E*, coimunoprecipitation of endogenous Lef-1 and Hmgn2. LS-8 epithelial cells were harvested, and Lef-1 Ab was used to pull down Hmgn2. Hmgn2 protein is shown by Western blot. CMV, cytomegalovirus; EYFP, enhanced YFP; HEK-293, human embryonic kidney 293 cell line; HMGN2, high mobility group protein N2.

HMGN2 inhibits Lef-1 DNA-binding activity

HMGN2 inhibits Lef-1 transcriptional activity through direct interactions in the cell nucleus. However, the mechanism for this inhibition is not known. We asked if HMGN2 inhibited Lef-1 DNA-binding activity because of its interaction with the Lef-1 HMG-box domain. Interestingly, titration of purified HMGN2 after Lef-1 binding to a labeled Lef-1-binding sequence (Lef-1 probe) in an EMSA showed that HMGN2 acts to inhibit Lef-1 binding to its DNA-binding element (Fig. 3). HMGN2 binds nonspecifically to the DNA probe as shown previously (23). Thus, HMGN2 can bind to Lef-1 bound to DNA and remove Lef-1 from the DNA. This represents a unique function of HMGN2 to regulate transcription factor activity.

Lef-1 and Pitx2 regulate the Hmgn2 promoter, and HMGN2 feeds back to inhibit Lef-1 and Pitx2 DNA binding, which is derepressed by β-cat

Because Lef-1 and Pitx2 are early developmental transcription factors and HMGN2 is expressed in early development, we asked if they regulated *HMGN2* expression. The *Hmgn2* promoter has several Lef-1- and Pitx2-binding sites (Fig. S1*A*). We cloned the *Hmgn2* promoter (11 kb) into a luciferase construct and transfected it with plasmid DNA encoding Lef-1, HMGN2, β-cat, and Pitx2 combinations in CHO cells. Our results showed that Lef-1 activates the *Hmgn2* promoter at approximately sixfold, and addition of HMGN2 represses Lef-1 activation as predicted (Fig. S1*B*). β-cat derepresses the HMGN2 inhibition of Lef-1 transcriptional activation of the *Hmgn2* promoter. Pitx2 activation of the *Hmgn2* promoter is also repressed by HMGN2 and derepressed by addition of β-cat (Fig. S1*B*). We have shown previously that β-cat can derepress Pitx2 inhibition by HMGN2 by forming a complex that allows for Pitx2 binding to DNA (23). We speculate that a similar mechanism is working for Lef-1 transcriptional activation. We assayed for endogenous *Hmgn2* transcripts isolated from E14.5 *Pitx2$^{-/-}$* null embryo mandibles and found that *Hmgn2* transcripts were significantly decreased because of the lack of Pitx2 expression (Fig. S1*C*). Thus, both Lef-1 and Pitx2 appear to regulate *Hmgn2* causing a new feedback mechanism where
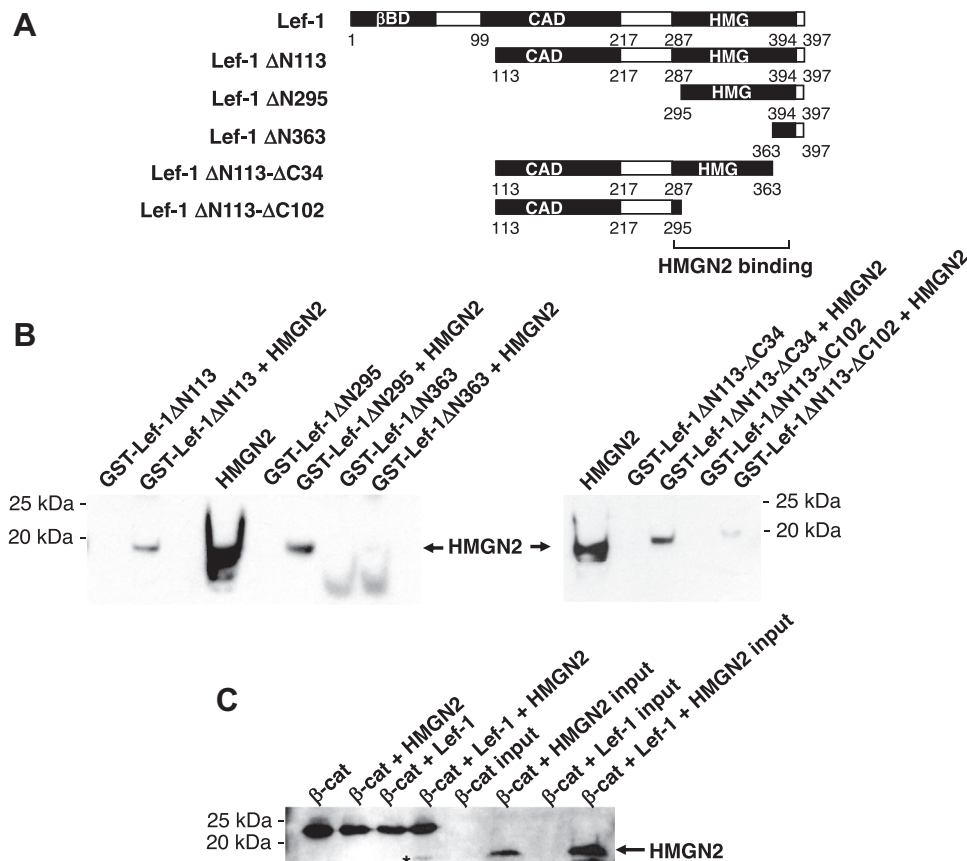
Figure 2. HMGN2 interacts with the HMG-box domain in the Lef-1 protein. *A*, schematic of the Lef-1 protein and truncated proteins. The location of the HMGN2-binding domain in the Lef-1 protein is shown. *B*, GST-Lef-1 protein pull-down assay with bacterial-expressed and purified HMGN2 protein (100 ng). To demonstrate HMGN2 binding to Lef-1, Lef-1 protein was incubated with purified HMGN2 protein. HMGN2 binds to the Lef-1 HMG domain. *C*, coimmunoprecipitation (IP) experiments demonstrate a Lef-1–HMGN2–β-catenin (β-cat) complex in CHO cells. Lef-1, HMGN2, and/or β-cat (2.5 μg) were transfected into CHO cells. Cell lysates were incubated with β-cat antibody (Ab), and the IP complex was isolated and resolved on a 10% SDS-polyacrylamide gel and probed for HMGN2 using the HMGN2 Ab. The β-cat antibody immunoprecipitated the Lef-1–HMGN2–β-cat complex, denoted by the *asterisk*. HMGN2 was detected only in the β-cat–Lef-1–HMGN2 precipitated complex. HMGN2 does not bind to β-cat. As controls transfected β-cat input, cotransfected β-cat and HMGN2, cotransfected β-cat and Lef-1, and all three cotransfected protein inputs were probed for HMGN2 protein. The proteins were visualized using ECL reagents. CHO, Chinese hamster ovary; GST, glutathione-*S*-transferase; HMGN2, high mobility group protein N2.

increased Hmgn2 protein would inhibit Pitx2 and Lef-1 activation of *Hmgn2* expression.

Dlx2 and FoxJ1 transcription factors are inhibited by HMGN2

Dlx2 and FoxJ1 are transcription factors involved in the developmental regulation of the craniofacial region and teeth (42–44). We asked if HMGN2 also regulated the transcriptional activity of these different Dlx and Fox family transcription factors. Both Dlx2 and FoxJ1 can activate their own promoter and are expressed in similar tissues with Hmgn2. The *Dlx2* promoter-luciferase construct was transfected into three cell lines (CHO, LS-8, and human embryonic kidney 293 [HEK-293] cell lines) with empty vector, HMGN2, Dlx2 or HMGN2 and Dlx2 together, and luciferase activity was measured as a readout of promoter activation (Fig. 4). Both empty vector control and HMGN2 expression did not activate the *Dlx2* promoter (Fig. 4*A*). However, Dlx2 activated the *Dlx2* promoter at approximately 10-fold in all cells, and HMGN2 repressed Dlx2 activation of the promoter in all cell lines (Fig. 4*A*). The *FoxJ1* promoter-luciferase construct was transfected in all cell lines as in panel *A*, with empty vector as a

control, HMGN2, FoxJ1, and both HMGN2 and FoxJ1 (Fig. 4*B*). Identical to the *Dlx2* promoter, FoxJ1 activated its own promoter, and HMGN2 alone had no effect on *FoxJ1* promoter activity. However, HMGN2 repressed FoxJ1 activation of the *FoxJ1* promoter in all cell lines (Fig. 4*B*). FoxJ1 and Dlx2 directly interact with Hmgn2. A co-IP was performed using either an antibody (Ab) to FoxJ1 or Dlx2 to pull down endogenous Hmgn2 in LS-8 cells. Endogenous FoxJ1 and Dlx2 directly interacted with Hmgn2 in the LS-8 cells (Fig. 4*C*). These data demonstrate that HMGN2 can repress the transcriptional activity of two different families of transcription factors.

miR-23a and miR-23b modulate HMGN2 expression

HMGN2 is required for tight regulation of several transcriptional activities to allow for normal craniofacial/tooth development (23, 39, 45). In this report, we show that Lef-1 and Pitx2 regulate the *Hmgn2* promoter; however, other mechanisms also regulate *Hmgn2* expression. To determine if miRs are potential regulators of *Hmgn2*, we analyzed the 3′UTR sequence of *Hmgn2* and found highly conserved
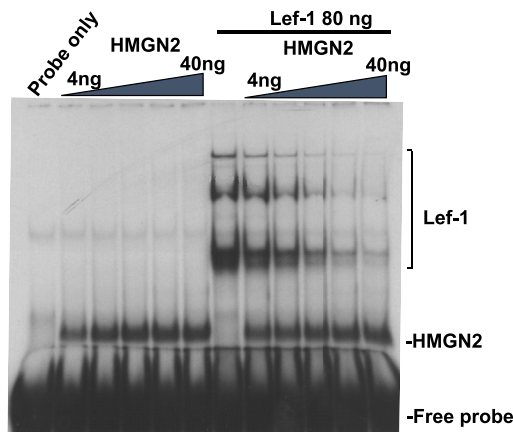
Figure 3. HMGN2 removes Lef-1 bound to DNA. HMGN2 protein (4, 10, 15, 20, and 40 ng) was incubated with the *Dlx2* promoter sequence containing a Lef-1 binding element as the radioactive probe in an EMSA. HMGN2 bound nonspecifically to the DNA probe as previously reported. Lef-1 protein (80 ng) bound to the DNA. HMGN2 titration (4, 10, 15, 20, and 40 ng) after Lef-1 bound to the probe revealed that HMGN2 inhibited Lef-1 binding in a dose-responsive manner. The EMSA experiments were analyzed in 8% native polyacrylamide gels. The free and bound forms of DNA were quantitated using the Molecular Dynamics STORM Phospholmager. The free probe and bound DNA are indicated. HMGN2, high mobility group protein N2.

miR-23a- and *miR-23b*-binding elements (Fig. 5A). To determine if *miR-23a* and *miR-23b* target *Hmgn2* expression in oral epithelial cells, we cloned the *Hmgn2* 3′UTR containing the *miR-23a* and *miR-23b*-binding site into a dual-luciferase reporter and transfected this reporter into LS-8 cells alone or with the constructs to overexpress *miR-23a* and/or *miR-23b*. The luciferase activity of WT *Hmgn2* 3′UTR was significantly repressed by the presence of either *miR-23a* or/and *miR-23b* (Fig. 5B). As controls, mutation of the conserved *miR-23a+b* binding site in the *Hmgn2* 3′UTR abolished the repression by *miR-23a+b* (Fig. 5C). Overexpression of *miR-23a* and *miR-23b* separately and together leads to reduced endogenous Hmgn2 protein expression in LS-8 cells (Fig. 5D). *miR-23a* and *miR-23b* target and repress *Hmgn2* expression. However, it is important to show that these miRs are coexpressed with *Hmgn2* in the craniofacial/tooth regions of mice during development.

miR-23a+b *indirectly activate* Pitx2 *and* amelogenin *expression by repressing* Hmgn2 *expression in dental epithelial cells*

To further understand the regulation of *Hmgn2* by *miR-23a+b* and the contribution to tooth organogenesis, we assayed for *miR-23a* and *miR-23b* expression in postnatal (P) P0 and P10 murine molars and incisors. We have previously shown that *Hmgn2* expression decreases in these tooth organs at later stages of development (39). Here, we show that *miR-23a+b* expression increases in P10 molars and incisors compared with P0 molars and incisors by miR microarrays (Fig. 6A). Pitx2 regulates *amelogenin* expression during tooth morphogenesis, and Pitx2 activates the *amelogenin* promoter (39). Here, we show that Pitx2 activation of the *amelogenin*

(*Amelo*) promoter is increased when *miR-23a* or *miR-23b* is coexpressed with Pitx2. HMGN2 can repress Pitx2 activation of the *amelogenin* promoter, and it appears that *miR-23* represses endogenous *Hmgn2* expression to allow for increased Pitx2 activation (Fig. 6B).

Endogenous *Hmgn2*, *miR-23a+b*, and *amelogenin* expression were analyzed during murine mandible/tooth development. RNA was isolated from murine E14.5, E16.5, E18.5, P0, P2, and P4 mandibles, including molars and incisors, and gene expression was determined by quantitative PCR (qPCR). Interestingly, *Hmgn2* expression decreases as *miR-23a+b* expression increases during early development (Fig. 6C). During this time, *amelogenin* expression increases correlating with amelogenesis and enamel formation (Fig. 6C). In the LS-8 dental epithelial cell line, the detection of Hmgn2 was verified by immunofluorescence and decreased in LS-8 cells overexpressing *miR-23b* (Fig. 6D). In contrast, *amelogenin* expression increased in LS-8 cells transduced with *miR-23b* (Fig. 6D). Transcripts for *miR-23b*, *Hmgn2*, and *amelogenin* were assayed by qPCR for their expression levels in these LS-8 cells. *miR-23b*-transduced cells had decreased levels of *Hmgn2* and increased levels of *amelogenin* transcripts (Fig. 6E). Thus, as *miR-23a+b* levels increase, the level of *Hmgn2* decreases, thereby allowing for *amelogenin* expression and enamel formation during tooth development.

miR-23a+b *inhibition of HMGN2 expression increases Dlx2 and FoxJ1 transactivation*

We demonstrated that HMGN2 represses the transcriptional activity of Dlx2 and FoxJ1 in Figure 4. To determine if *miR-23a+b* expression could also increase Dlx2 and FoxJ1 transactivation of their promoters, we assayed for transcriptional activity in three cell lines. As a control, the *Dlx2*-luciferase promoter construct was transfected with empty vector and *miR-21*, which did not affect promoter activation or Dlx2 activation of the promoter (Fig. S2A). Cotransfection of *miR-23a* and/or *miR-23b* with Dlx2 significantly increased activation of the *Dlx2* promoter in all cell lines (Fig. S2A). Similar results are shown for FoxJ1 activation of the *FoxJ1*-luciferase promoter construct in the presence of *miR-23a* and/or *miR-23b* (Fig. S2B). These results again are consistent with our hypothesis that *miR-23* directed inhibition of endogenous *Hmgn2*, which increases the transcriptional activation of these two transcription factors.

These experiments were repeated in WT mouse embryo fibroblasts (MEFs) and HMGN2 overexpression transgenic (TG) MEFs. We have previously reported on the phenotype and gene regulation of mice overexpressing HMGN2 (39). In these experiments, we asked if *miR-23* inhibition of endogenous Hmgn2 and overexpression of *HMGN2* in MEFs affected Pitx2 activation of the *Lef-1* promoter (Fig. S3A). The *Lef-1* promoter-luciferase construct was cotransfected into WT and *HMGN2-TG* (TG mice overexpressing *HMGN2*) (39) MEFs with Pitx2 and *miR-23a* and *miR-23b*. *miR-21* was transfected as a control. The miRs alone had no effect on *Lef-1* promoter activity (Fig. S3A).
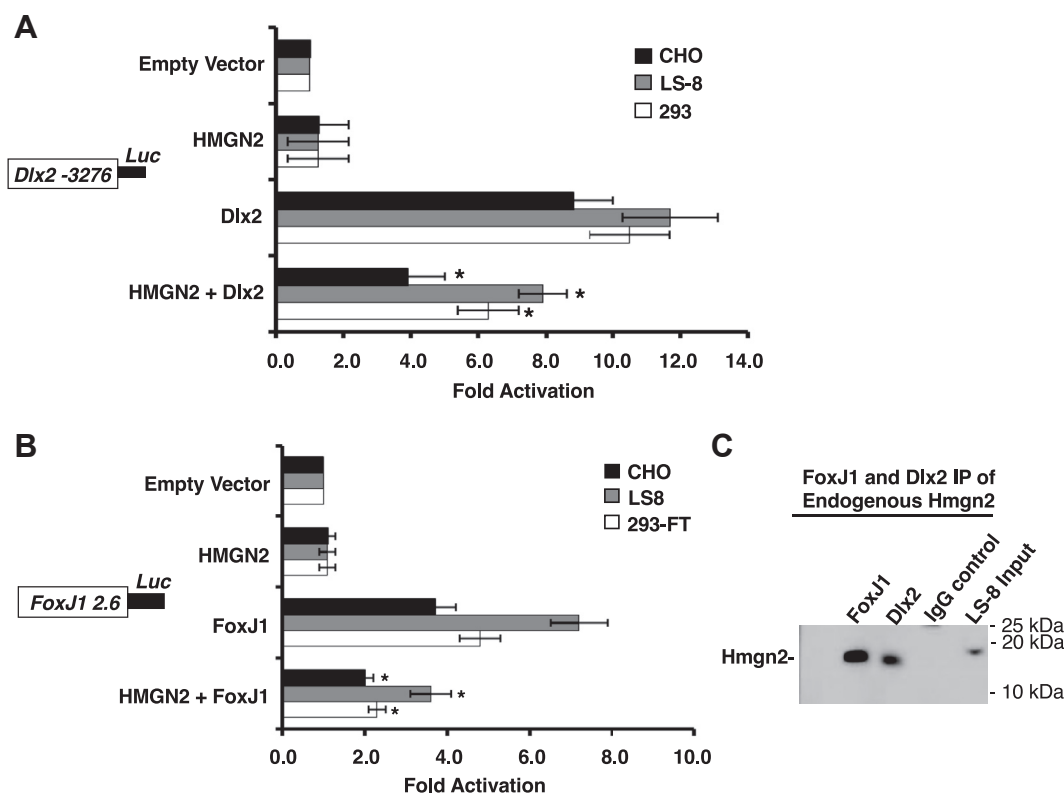
Figure 4. HMGN2 represses Dlx2 and FoxJ1 transcriptional activation. *A*, CHO, LS-8, and 293 cells were cotransfected with the *Dlx2* luciferase promoter (5 μg) construct, either Dlx2, HMGN2, or HMGN2 and Dlx2 expression constructs (2.5 μg). β-galactosidase expression construct (0.5 μg) was transfected to control for transfection efficiency. After 48 h, luciferase and β-galactosidase activities were measured. The luciferase activities are shown as mean fold activation compared with the normalized luciferase activity using an empty vector (pcDNA 3.1) with *Dlx2* promoter reporter. *B*, CHO, LS-8, and 293 cells were cotransfected with the *FoxJ1* luciferase promoter construct, FoxJ1, HMGN2, or HMGN2 and FoxJ1 expression constructs (2.5 μg). β-galactosidase expression construct (0.5 μg) was transfected to control for transfection efficiency. Experiments were performed as in *A*. N = 4, *$p < 0.05$. *C*, coimmunoprecipitation of endogenous FoxJ1, Dlx2, and Hmgn2. LS-8 epithelial cells were harvested, and FoxJ1 Ab or Dlx2 Ab was used to pull down Hmgn2. Hmgn2 protein is shown by Western blot. CHO, Chinese hamster ovary; HMGN2, high mobility group protein N2.

Pitx2 activated the *Lef-1* promoter at threefold in WT MEFs, and this activation was reduced in MEFs over-expressing HMGN2. Cotransfection of *miR-21* as a control miR with Pitx2 had no effect on Pitx2 activation of the *Lef-1* promoter in both WT and *HMGN2-TG* MEFs. Cotransfection of *miR-23a*, *miR-23b*, and both *miR-23a+b* significantly increased Pitx2 activation of the *Lef-1* promoter in both WT and *HMGN2-TG* MEFs (Fig. S3A). Thus, *miR-23* was able to inhibit endogenous *Hmgn2* expression and facilitate Pitx2 activation of the *Lef-1* promoter. The *HMGN2* construct used to make the *HMGN2-TG* mice lacks a 3′UTR and is not regulated by any miRs, and the increase in Pitx2 activation is due to inhibition of endogenous Hmgn2. Thus, the exogenous levels of HMGN2 in the *HMGN2-TG* MEFs cause a reduced inhibition of the transcription factors compared with WT.

The same *miR-23* effect is shown for Dlx2 activation of the *Dlx2* promoter (Fig. S3B) and FoxJ1 activation of the *FoxJ1* promoter in both WT MEFs and *HMGN2-TG* MEFs (Fig. S3C). These data demonstrate that HMGN2 over-expression in MEFs represses the activity of three well-known developmentally regulated transcription factors. Furthermore, *miR-23* regulation of *Hmgn2* expression indirectly regulates the activity of these important development factors.

H4K5ac and H3K4me2 chromatin factors associate with Pitx2 and Hmgn2 near the *Dlx2* transcription start site

HMGN2 has been shown to bind to DNase I DNA-hypersensitive sites and maintain and open chromatin structure (4, 46). Both H4K5ac and H3K4me2 epigenetic factors are associated with open chromatin at transcription start sites (TSSs) and proximal promoter regions (47, 48). A triple chromatin immunoprecipitation (ChIP) assay was performed, first using the H4K5ac Ab to pull down chromatin bound by this factor, and immunoglobulin G (IgG) only did not immunoprecipitate the initial complex. The complex was washed and followed by a second IP using the Hmgn2 Ab with control IP and a third IP using the Pitx2 Ab with control IP in LS-8 cells. After reverse crosslinking, a qPCR using primers to the indicated proximal *Dlx2* promoter sequence amplified a 390 bp product (Fig. S4, *A* and *B*; lane 2). Chromatin input is shown in lane 4. As controls, Dlx2 primers alone (lane 3), IgG Ab IP and Dlx2 primers (lane 5), and Pitx2, Hmgn2, and H4K5ac Ab IP with control primers to an upstream region of the *Dlx2* promoter were used (Fig. S4B, lane 6). A similar triple ChIP experiment was performed first using the H3K4me2 Ab, followed by the Hmgn2 Ab, and finally with the Pitx2 Ab in LS-8 cells. The indicated proximal *Dlx2* promoter sequence was amplified
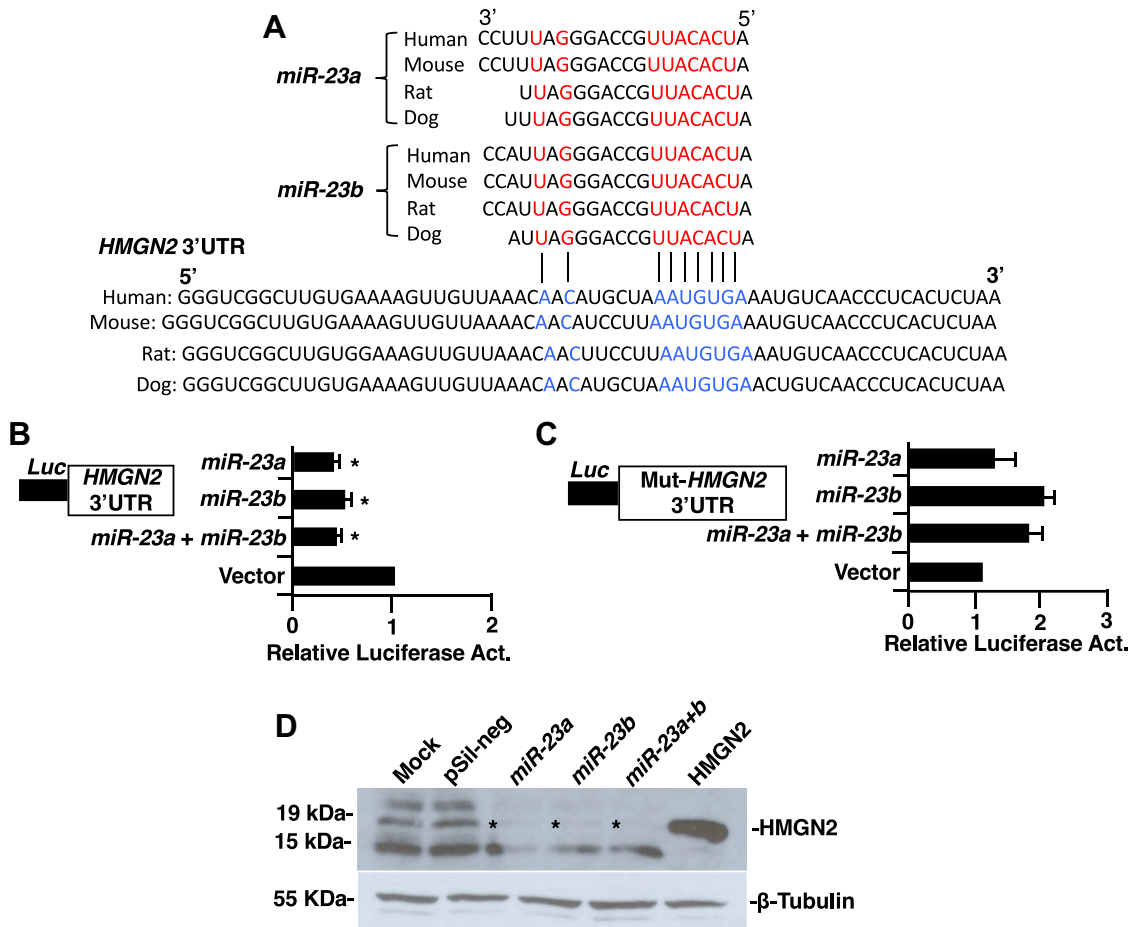
Figure 5. *miR-23a* and *miR-23b* target HMGN2. *A, miR-23a* and *miR-23b* are evolutionarily conserved among several vertebrate species, and the potential *miR-23a* and *miR-23b* binding sites in the *Hmgn2* 3′-UTR are highly conserved among different species. *B, miR-23a* and *miR-23b* directly target the *Hmgn2* 3′-UTR. *Hmgn2* 3′-UTR pGL3 reporter (1 μg) and 2.5 μg pre-*miR-23a* or *miR-23b* or empty vector (pSil) were transfected into LS-8 cells. Cells were incubated for 48 h and then assayed for luciferase and β-galactosidase activities. *C, miR-23a* and *miR-23b* do not target the *Hmgn2* 3′ UTR with mutations engineered in the region complementary to the *miR-23a* and *miR-23b* seed region. The activities are shown in *B* and *C* as mean fold activation compared with luciferase activity with an empty vector (pSil) and normalized to β-galactosidase activity. N = 3, *$p < 0.05$. *D, miR-23a* and *miR-23b* repress endogenous HMGN2 expression. Western blot of Hmgn2 protein in control or *miR-23a* or/and *miR-23b* precursor transfected LS-8 cells 48 h post-transfection. β-tubulin is shown as a loading control. Mock, pSil-neg vector served as controls. HMGN2, high mobility group protein N2.

using the specific primers (Fig. S4C, lane 2). Chromatin input is shown in lane 4. As controls, Dlx2 primers alone and IgG Ab IP with Dlx2 primers are shown (Fig. S4C, lanes 3 and 5, respectively). While there are multiple Pitx2-binding sites in the *Dlx2* promoter sequence, we have previously reported that when Pitx2 is bound to HMGN2, Pitx2 is not bound to DNA, but upon interaction with Wnt signaling and direct interaction with β-cat, Pitx2 is released from chromatin-bound HMGN2, and Pitx2 binds directly to TAATCC-binding elements in specific promoters (23). Thus, we show that Hmgn2, which is bound to chromatin (marked by H4K5ac and H3K4me2), binds to Pitx2 in a chromatin complex (23).

Hmgn2 is developmentally regulated and controls dental epithelial cell proliferation

Hmgn2^{+/−} mice expressing LacZ were X-gal stained, and whole embryos from E10.5 to P0 were analyzed by light microscopy (Fig. 7A). *Hmgn2* LacZ has high expression levels during early developmental stages and gradually decreases prior to birth. These data are consistent with our previous report showing that *Hmgn2* transcripts decrease during later embryonic stages (39). We study craniofacial and tooth development, and a diagram of the developing lower incisor at E16.5 is shown depicting the lingual cervical loop and labial cervical loop (LaCL) and dental epithelia (Fig. 7B). Hmgn2 is expressed in the developing murine lower incisor at E14.5 (Fig. 7C) but is absent from the *Hmgn2*^{−/−} E14.5 embryos (Fig. 7D).

We next determined if dental epithelial cell proliferation was affected in the lower incisor of *Hmgn2*^{−/−} embryos. We have previously shown that Pitx2 and Lef-1 control dental epithelial cell proliferation and differentiation (24, 25, 49). Our hypothesis is that the loss of *Hmgn2* would increase the transcriptional activity of factors involved in dental epithelial cell proliferation and differentiation. Immunofluorescence staining of the cell proliferation marker, Ki67, was performed
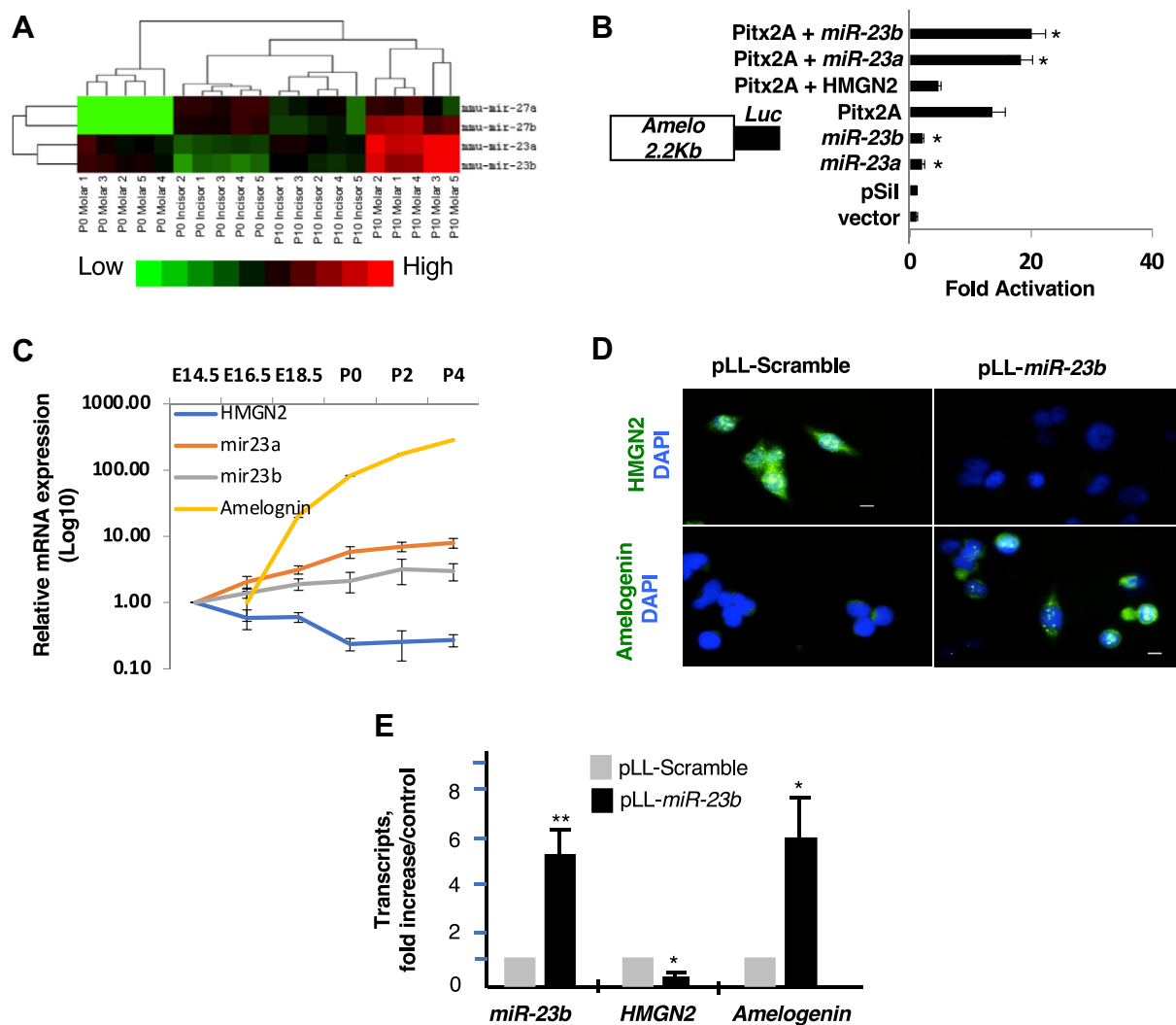
Figure 6. *miR-23a+b* expression correlates with developmental time points and amelogenin expression. *A*, microRNA microarrays of murine molar and incisor dental epithelium from five biological replicates at P0 and P10 WT embryos show an increase in *miR-27* and *miR-23* expression at later stages of development. *B*, transfection of LS-8 cells was performed with the amelogenin (Amelo) luciferase reporter (5 µg), Pitx2, HMGN2, *miR-23a*, and *miR-23b* (2.5 µg) expression plasmids. Transfection analyses were performed as previously described (Figs. 4 and 5). N = 3, *$p < 0.05$. *C*, RNAs isolated from E14.5, E16.5, E18.5, P0, P2, and P4 murine mandibles were analyzed by quantitative PCR (qPCR) for *HMGN2*, *miR-23a*, *miR-23b*, and *amelogenin* transcript levels. Relative levels of each transcript are shown. *D*, LS-8 cells transduced with lentivirus expressing *miR-23b* or a scrambled control were analyzed for Hmgn2 and amelogenin expression by immunofluorescence. LS-8 cells expressing *miR-23b* did not express Hmgn2; however, amelogenin was expressed in these cells compared with control cells. The scale bars represent 50 µm. *E*, RNA isolated from the LS-8 cells and analyzed by qPCR for *Hmgn2*, *miR-23b*, and *amelogenin* transcript levels. Relative levels of each transcript are shown. N = 3, *$p < 0.05$; **$p < 0.01$. HMGN2, high mobility group protein N2.

in sagittal sections of E16.5 and P0 *Hmgn2*$^{-/-}$ and WT murine lower incisors. E16.5 *Hmgn2*$^{-/-}$ embryos revealed an increase in progenitor cell and transient amplifying cell (TAC) proliferation in the LaCL (stem cell niche) and lingual cervical loop compared with WT embryos (Fig. 7, *E* and *F*). At P0 dental epithelial cell, proliferation is mainly confined to the TAC region in WT embryos (Fig. 7, *G* and *H*). However, in the P0 *Hmgn2*$^{-/-}$ embryos, cell proliferation was present in the LaCL (Fig. 7,*I* and *J*). In normal incisor development and growth, cells exit the LaCL, migrating to the TAC region, where they proliferate and begin differentiation to ameloblast cells. Quantitation of Ki67+ cells in the dental epithelium shows an increase in proliferative cells (Fig. 7*K*). The lack of Hmgn2 protein appears to stimulate premature and prolonged cell proliferation in the LaCL.

HMGN2$^{-/-}$ murine incisors have increased amelogenin and enamel formation

To investigate if dental epithelial cell gene expression was affected in *Hmgn2*$^{-/-}$ murine incisors, we analyzed several markers of dental epithelium. E-cadherin, highly expressed in undifferentiated dental epithelium (50), remained unchanged between WT and *Hmgn2*$^{-/-}$ incisors (data not shown). Amelogenin, which is the most abundant (90%) enamel matrix protein and critical for enamel development, is normally expressed in secretory stage ameloblasts in the anterior region of incisor at P0 (Fig. 8, *A* and *C*). However, amelogenin expression was expanded toward the posterior (Pos) region of the incisors in *Hmgn2*$^{-/-}$ mice, suggesting ablation of *Hmgn2* results in increasing/expanded amelogenin expression in teeth (Fig. 8, *B* and *D*). Trichrome staining at the P4 stage to mark
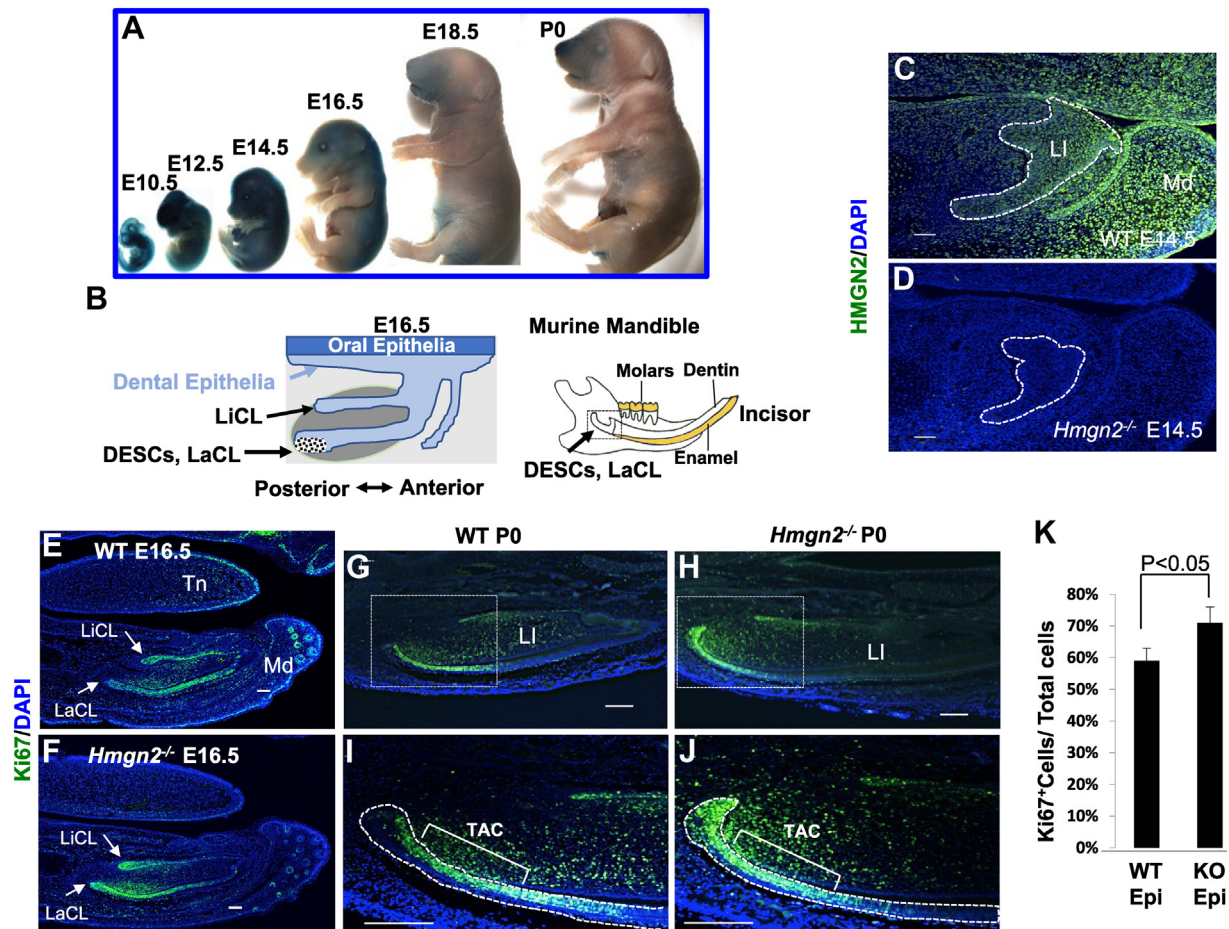
Figure 7. HMGN2 LacZ expression decreases during development and regulates cell proliferation. *A, Hmgn2*^{+/−} whole embryos expressing LacZ were stained for X-gal expression and visualized by light microscopy. *B*, diagram of murine *lower incisor* development at E16.5 and the mature murine mandible. *C* and *D*, WT and *Hmgn2*^{−/−} E14.5 embryo *lower incisor* sections were incubated with Hmgn2 antibody (Ab) and visualized using a secondary immuno-fluorescence Ab to detect Hmgn2 expression. *E* and *F*, E16.5 WT and *Hmgn2*^{−/−} embryo *lower incisor* sections, respectively, were incubated with Ki67 Ab and visualized using a secondary immunofluorescence Ab to detect Ki67 expression. *G* and *H*, P0 WT and *Hmgn2*^{−/−} embryo lower incisor sections, respectively, were incubated with Ki67 Ab and visualized using a secondary immunofluorescence Ab to detect Ki67 expression. The regions denoted by the *dotted square* were magnified (*I* and *J*) to show the LaCL and transient amplifying cell (TAC) region. The scale bars represent 100 μm. *K*, quantification using ImageJ of Ki67+ cells shows an increase in cell proliferation in the *Hmgn2* KO embryos. DESC, dental epithelial stem cell; HMGN2, high mobility group protein N2; LaCL, labial cervical loop; LI, lower incisor; LiCL, lingual cervical loop; Md, mandible; Tn, tongue.

the enamel and dentin in incisors also revealed that the enamel layer in *Hmgn2*^{−/−} mice was expanded posteriorly compared with WT (Fig. 8, *E–H*). These data showing increased amelogenin expression and enamel formation in *Hmgn2*^{−/−} mice are consistent with Hmgn2 acting as a repressor for Pitx2, Lef-1, Dlx2, and FoxJ1 activation of amelogenin expression. In addition, dentin sialo phosphoprotein (DSPP) was increased in the posterior preameloblast region of the P2 *Hmgn2*^{−/−} incisors (Fig. 8,*I* and *J*). DSPP is transiently expressed in the ameloblasts cells and mainly confined to odontoblasts. Consistent with an increase in cell proliferation and amelogenin expression in the posterior region of the incisor, increased DSPP expression may also indicate an increase in cell differentiation in the anterior region of the *Hmgn2*^{−/−} lower incisor.

Discussion

In this report, we demonstrate the role of HMGN2 in regulating transcription factor activity and gene expression.

We first reported the ability of HMGN2 to bind Pitx2, a developmentally regulated homeodomain transcription factor (10). HMGN2 can remove Pitx2 from bound DNA to form an inactive transcriptional complex. We demonstrated that upon interaction with β-cat, the Pitx2–β-cat complex binds to Pitx2 enhancer elements to activate transcription (10). We proposed that HMGN2 binds to open chromatin complexed with Pitx2 poised to activate transcription when Wnt signaling is active (10). In a subsequent report, we demonstrated a role for HMGN2 in tooth development using a *Krt-14* promoter–driven *HMGN2* overexpression TG mouse (39). We now show that HMGN2 regulates several developmentally regulated transcription factors and that HMGN2 can regulate Lef-1 DNA binding similar to Pitx2. In addition, we analyzed the *Hmgn2*^{−/−} embryos for defects in tooth development.

More recent publications describe the conformation changes in the nucleosomes upon binding of HMGN1 and HMGN2 (2). HMGN2 binding to nucleosomes causes
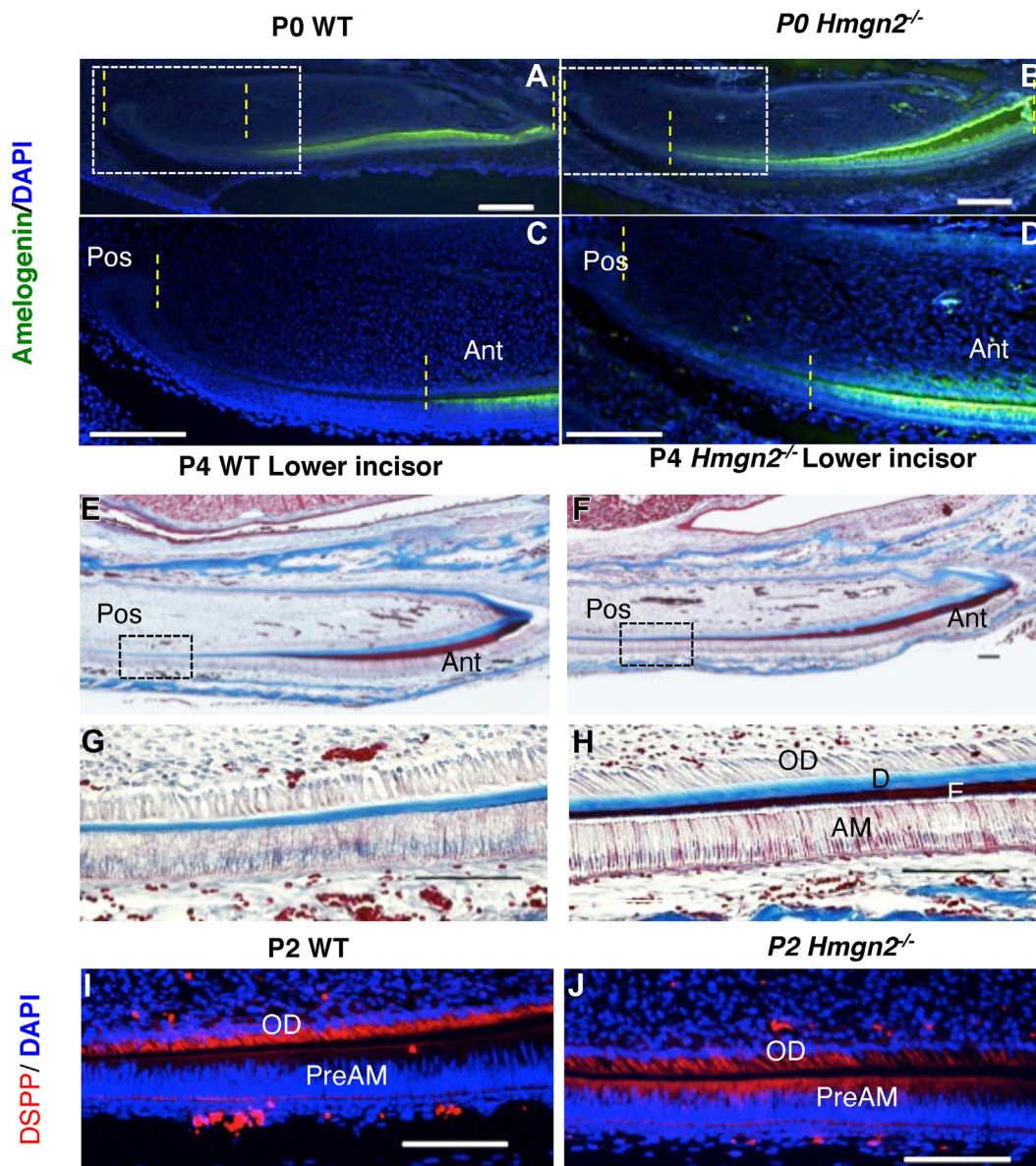
Figure 8. *Hmgn2*^{−/−} incisors have increased amelogenin expression and enamel formation. *A* and *B*, amelogenin immunofluorescence staining in lower incisors from P0 WT and *Hmgn2*^{−/−} mice. *C* and *D*, magnified images from *boxed region* in *A* and *B* highlight the amelogenin expression in presecretory ameloblast. Note that amelogenin expression moved further proximally in the incisors in *Hmgn2*^{−/−} mice. *E* and *F*, images of trichrome-stained *lower incisors* from P4 WT and *Hmgn2*^{−/−} mice, respectively. Note, the enamel was stained as *dark red*, and dentin was stained as *blue*. *G* and *H*, higher magnified pictures of *boxed regions* in *E* and *F*. In P4 *Hmgn2*^{−/−} mice, enamel deposition occurs more proximally in the incisor. *I* and *J*, immunofluorescence staining of Dspp in P2 WT and *Hmgn2*^{−/−} mice, respectively. Nuclei are counterstained with DAPI. The scale bars represent 100 μm AM, ameloblast; D, dentin; DAPI, 4′,6-diamidino-2-phenylindole; Dis, distal; Dspp, dentin sialo phosphoprotein; *E*, enamel; HMGN2, high mobility group protein N2; OD, odontoblast; preAM, presecretory ameloblast; Pro, proximal.

rearrangements of core and linker histone tail interactions leading to a less condensed chromatin structure (2, 4, 51, 52).

HMGN2 regulates Lef-1 DNA binding and transcriptional activity through an interaction with the Lef-1 HMG-box domain

Many reports have shown that either HMGN proteins or proteins containing HMG-binding domains act through protein interaction or chromatin-binding domains (1, 10, 24, 39, 45, 51, 53–56). We demonstrate that Lef-1, a HMG-box domain–containing transcription factor, directly interacts

with HMGN2 in the cell nucleus, using a BiFC assay. This interaction represses Lef-1 transcriptional activation of gene expression. We further demonstrate that similar to Pitx2 the repressive effect of HMGN2 on Lef-1 transcriptional activity is relieved by cotransfection of β-cat. We show that the HMG-box domain of Lef-1 directly interacts with HMGN2. IP experiments further show that HMGN2 interacts with a Lef-1−β-cat protein complex.

We identified a unique function of HMGN2 in its ability to bind to and remove Lef-1 from DNA, similar to its interaction with Pitx2 (10). Titration of HMGN2 protein in an EMSA experiment to Lef-1 bound to DNA effectively removed Lef-1

from DNA (Fig. 3). There are very few proteins with this molecular function, and HMGN2 appears to tightly control the transcriptional activity of several factors by this mechanism.

Interestingly, both Lef-1 and Pitx2 activate the *Hmgn2* promoter, and HMGN2 represses their transactivation activity as expected. Addition of β-cat derepresses the action of HMGN2 and restores the transcriptional activity of these factors. This corroborates our previous finding that HMGN2 forms an inactive transcriptional complex with transcription factors and upon Wnt signaling and interaction with β-cat converts the inactive complex to an active transcriptional complex (10).

HMGN2 regulates the transcriptional activity of multiple factors

HMGN2 has been reported to interact with other proteins but not at the transcriptional level. Because Lef-1 transcriptional activity was shown to be regulated by HMGN2, two other developmentally regulated transcription factors were also shown to be repressed by HMGN2 in promoter assays. Both Dlx2 and FoxJ1 are transcription factors involved in craniofacial and tooth development (40–42, 44, 57). Both genes play major roles in tissue-specific development and embryogenesis. Furthermore, Hmgn2 is considered a major regulator of the timing of early embryonic development in the mouse (11). Hmgn2 repression of Dlx2 and FoxJ1 is cell independent as three different cell lines were used to demonstrate the repressive effect of Hmgn2 on Dlx2 and FoxJ1 activity.

HMGN2 expression is controlled by miRs

Hmgn2 expression occurs during early mouse embryogenesis, and this expression decreases as development proceeds (12, 39, 54, 58). Hmgn2 is highly expressed throughout the entire embryo and decreased at birth. Several mechanisms could explain that *Hmgn2* reduced expression as embryonic development ends, including post-transcriptional epigenetic factors. miRs are involved in the modulation of temporal-spatial gene expression, and we show that as *miR-23* expression increases, *Hmgn2* expression decreases. *miR-23* indirectly regulates genes that are directly controlled by HMGN2 by binding to the *HMGN2* 3′UTR. We demonstrate a new mechanism for controlling gene expression during development where HMGN2 regulates multiple transcription factors required for several developmental processes. However, mechanisms are required to derepress the activity of Hmgn2 to activate transcription factors required for normal embryonic development. Thus, the expression of *miR-23* is required to allow for dental epithelium cell differentiation by repressing *Hmgn2* expression (Fig. 9A).

HMGN2 associates with open chromatin and the Pitx2 transcription factor to activate gene expression

HMGN proteins have emerged as essential regulators of transcription. Their interactions with nucleosomes and histones to regulate chromatin structure and the rates of transcription are required for development (1, 6–9, 51, 56, 59, 60). How these HMGN proteins recruit and activate gene expression remains unresolved, and our research provides an initial understanding of their transcriptional mechanisms. At the proximal promoter, two chromatin factors (H4K5ac and H3K4me2) are shown to be deposited and associated with active transcription (47, 48). These epigenetic factors are associated with transcription factor–binding regions. We demonstrate that the Hmgn2–Pitx2 complex is associated with either H4K5ac or H3K4me2 in a transcription factor–binding region poised to activate transcription (Fig. S4). It is well known that HMGN2 binds to histones and linker tails to open chromatin. Thus, we propose that the interaction of HMGN2 with chromatin, epigenetic marks, and transcription factors recruits the transcription factor to transcription factor–binding regions in open chromatin ready to activate gene expression upon stimuli such as Wnt/β-cat signaling (Fig. 9B) (10).

Pitx2 and Lef-1 activate HMGN2, and HMGN2 feeds back to repress their transcriptional activities
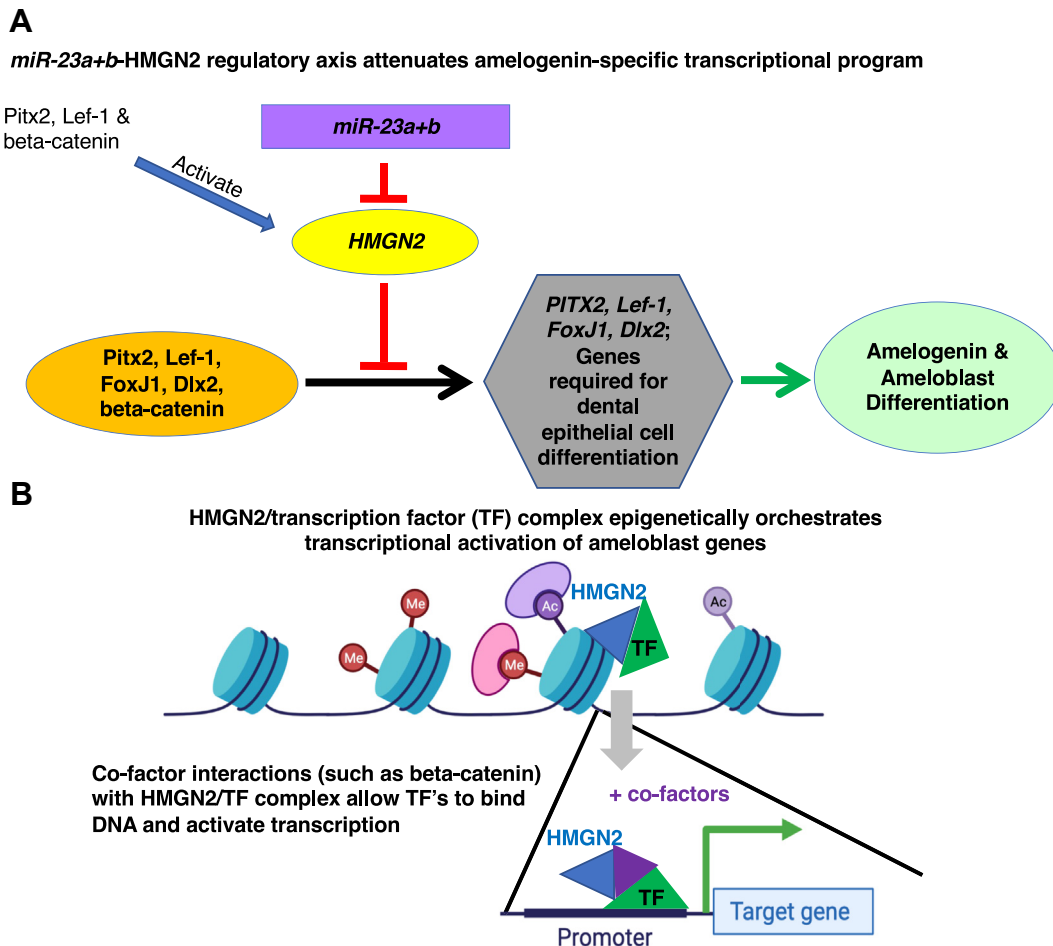
HMGN2 expression is differentially regulated during development as it is highly expressed during early tooth development and morphogenesis. HMGN2 acts to repress the transcriptional activities of genes during these early stages of progenitor cell proliferation, so these progenitor cells do not prematurely differentiate. However, as development proceeds, HMGN2 must be downregulated to generate the different stages of ameloblast differentiation and amelogenin expression to form enamel and the mature tooth. At later stages, *miR-23* expression increases to repress HMGN2, which allows for Pitx2, Lef-1, Dlx2, and FoxJ1 to activate genes required for ameloblast differentiation. HMGN2 plays a unique role in regulating the switch between proliferation and differentiation by directly interacting with and modulating the transcriptional activity of several genes.

HMGN2 is required for normal tooth development

HMGN2 modulates genes required for tooth development and differentiation as shown previously and, in this report, (39). Hmgn2 expression is developmentally regulated and modulates both cell proliferation in the murine lower incisor as well as amelogenin and Dspp expression. Amelogenin is required for enamel formation, and an increase in enamel formation was observed in the *Hmgn2*-null mice as well as an increase in Dspp expression. Thus, it appears that Hmgn2 controls cell differentiation in the lower incisor by regulating Dlx2, Pitx2, Lef-1, and FoxJ1 transcription factors, which are all known to regulate epithelial cell differentiation and amelogenesis (39–42, 44, 57).

These data demonstrate a unique role for Hmgn2 in the development of enamel formation through the regulation of multiple transcription factors. Furthermore, we have identified a new role for *miR-23* and epigenetic marks in modulating Hmgn2 activity. The early embryonic expression of Hmgn2 suggests that it plays a role in modulating transcription factor

A

miR-23a+b-HMGN2 regulatory axis attenuates amelogenin-specific transcriptional program

B

HMGN2/transcription factor (TF) complex epigenetically orchestrates transcriptional activation of ameloblast genes

Figure 9. Models for the role of HMGN2, chromatin marks and *miR-23a+b* in the regulation of gene expression. *A*, a feedback loop occurs where Pitx2, Lef-1, and β-catenin activates HMGN2 expression and then represses HMGN2 Pitx2 and Lef-1 transcriptional activity as well as other factors, *miR-23* expression allows for the repression of HMGN2 expression so transcription factors can activate tissue-specific genes. This mechanism fine tunes HMGN2 expression during development. Pitx2, Lef-1, FoxJ1, Dlx2, and β-catenin regulate genes required for dental epithelial cell differentiation, amelogenin expression, and ameloblast differentiation, which, leads to enamel mineralization. However, HMGN2 represses the transcriptional activity of these factors, and *miR-23a+b* then acts at later stages of development to repress HMGN2 expression and facilitate enamel formation. *B*, inactive HMGN2/Pitx2 transcription factor (TF) complex binds to H4K5ac and/or H3K4me2 histone marks in the chromatin. Specific cofactors release the inactive complex from chromatin as an active complex, which can bind specifically to DNA enhancers and activate transcription of target genes (10). HMGN2, high mobility group protein N2.

activity during developmental stages. Hmgn2 may orchestrate the ability of multiple factors to regulate gene expression in a temporal–spatial mechanism. Interestingly, after birth, Hmgn2 is downregulated and does not appear to be required for homeostasis. We show a role for Hmgn2 during tooth development; however, it is also required for other tissue/organ development. We speculate that the gene expression mechanisms reported in these experiments are also important for other tissue/organ developmental mechanisms.

Experimental procedures

Mouse strain breeding

All animals were housed, and all procedures were performed in accordance with the guidelines approved by the University of Iowa Office of Animal Care. All experimental procedures were approved in accordance with the University

of Iowa Institutional Animal Care and Use Committee guidelines. The $Hmgn2^{-/-}$ mice were generated from ($Hmgn2^{tm1b(KOMP)Wtsi}$) knockout embryonic stem cells obtained from KOMP repository. The *Pitx2* TG mouse was previously described (39).

miR microarray

Incisor and molar tooth germs were dissected from P0 and P10 mice using a dissection microscope. To separate epithelium and mesenchyme, the tooth germs were treated with dispase II and collagenase I (Worthington) for 30 min at 37 °C. This procedure separates the epithelium from the mesenchyme and allows for specific RNA extraction of the two tissue types (31). Total RNAs including miR were prepared using miRNeasy Mini Kit from Qiagen. LC Sciences performed the miR microarray analyses.

BiFC assay

The BiFC assay was performed as previously reported (38). *Lef-1* complementary DNA was cloned into the pFLAG-CMV-2 plasmid (Sigma) containing an N-terminal fragment of EYFP, and *HMGN2* was ligated to a C-terminal fragment of EYFP in the pFLAG-CMV-2 plasmid as shown in Figure 1*A*. YN or YC fragments only were ligated into the vector and used as negative controls. One microgram of each construct was transfected into HEK-293 cells. After 24 h, Nikon 80i fluorescence microscope was used to detect the fluorescence.

Fluorescence immunocytochemistry

Approximately 5000 cells were seeded on glass slides 24 h prior to fixation. The slides were washed in 1× PBS and then incubated in ice-cold acetone for 5 min at 4 °C. Fixed cells were washed twice with PBS with Tween 20 (PBST) (5 min each). Subsequently, the slides were incubated in 10% normal goat serum–PBST for 30 min at room temperature for blocking. Slides were then incubated with either amelogenin Ab (Santa Cruz; 1:500 dilution), KI67 Ab (Abcam; 1:500 dilution), or HMGN2 Ab (Cell Signaling; 1:5000 dilution) at 4 °C overnight. Cells were rinsed with PBST three times, 10 min each, and were incubated with goat anti-rabbit Alexa-488-labeled secondary Ab (Invitrogen) for 30 min at 37 °C. Finally, the cells were washed with PBST three times, 10 min each, and counterstained using a mounting solution containing 4′,6-diamidino-2-phenylindole.

LacZ staining

Embryos or postnatal pups of different stages were fixed for 20 to 40 min at room temperature in the fix solution (0.2% glutaraldehyde, 2% formaldehyde, 2 mM $MgCl_2$, 5 mM EDTA [pH 8.0], and 100 mM NaH_2PO_4 [pH 7.3]) and washed three times in rinse solution (0.2% Nonidet P-40 and 0.1% sodium deoxycholate, 100 mM NaH_2PO_4 [pH 7.3], and 2 mM $MgCl_2$). Embryos were stained for 24 to 48 h at 37 °C in staining solution (1.65 mg/ml potassium ferricyanide, 1.84 mg/ml potassium ferrocyanide, 2 mM $MgCl_2$, and 1 mg/ml X-gal in rinse solution), rinsed in PBS, and postfixed in 4% paraformaldehyde (PFA).

Histology, fluorescent immunohistochemistry, and trichrome staining

Murine embryos or postnatal pups were used for histology and fluorescence immunohistochemistry. Samples were fixed in 4% PFA, dehydrated, and embedded in paraffin. Sections were cut to 7 μm thickness and standard hematoxylin and eosin staining to assess tissue morphology. Sections that were used for fluorescence immunohistochemistry were rehydrated and treated with 10 mM sodium citrate solution for 20 min at a slow boil for antigen retrieval. These sections were incubated with 10% goat serum–PBST for 30 min at room temperature, followed by overnight incubation at 4 °C with an Ab against one of the following proteins: amelogenin (Santa Cruz; 1:200 dilution), Hmgn2 (Millipore; 1:500 dilution), Ameb (Santa Cruz; 1:200 dilution), Enml (Santa Cruz; 1:200 dilution), Ki67

(Abcam; 1:250 dilution), E-cadherin (BD Bioscience; 1:200 dilution), or Dspp (Santa Cruz; 1:200 dilution). After the incubation, the slides were treated with Alexa-488 (FITC channel) or Alexa-555 (Cy3 channel)–labeled secondary Ab (Invitrogen) at a concentration of 1:500 for 30 min. Each Ab incubation was followed by 3 to 6 PBST washes. Nuclear counterstaining was performed by applying a 4′,6-diamidino-2-phenylindole–containing mounting solution after the final wash (Vector Laboratories). The trichrome staining was carried out as previously described (31). Samples were stained with azocarmin for 1 h at 50 °C and then stained with aniline to differentiate nuclei. Finally, samples were stained with Orange G and Aniline blue for 2 h.

Expression and luciferase reporter constructs

Pitx2A, *Pitx2C*, and *HMGN2* complementary DNA were cloned into pcDNA-3.1-MycHisC (Invitrogen) using cytomegalovirus (CMV) promoter to allow expression in eukaryotic cells. *miR-23a* and *miR-23b* were cloned into pSilencer 4.1 (Life Technologies). A 5.3 kb upstream of *Pitx2* TSS and 2.2 kb upstream of *amelogenin* TSS were cloned into pTK-Luc vectors to generate the promoter luciferase reporters.

The *Hmgn2* 3′UTR was ligated to downstream of a luciferase gene in pGL3 reporter vector (Promega). PCR-driven overlap extension method was used to mutate the *miR23-a/b*–binding site in *Hmgn2* 3′UTR (AAUGUGA to CCGAGAC). β-cat, Foxj1, Dlx2, Lef-1, Pitx2, and HMGN2 expression constructs have been previously reported (10, 22, 23, 40, 42, 44). All the cloned constructs were confirmed by DNA sequencing. All plasmids used for transfection were purified by double banding in cesium chloride.

Cell culture, transfections, and reporter assays

LS-8 (61), HEK-293, and CHO cells were cultured in Dulbecco's modified Eagle's medium supplemented with 10% fetal bovine serum and 1% penicillin/streptomycin and transfected by electroporation. MEFs were isolated and cultured from E16.5 WT and *HMGN2* TG embryos. Cells were resuspended in PBS and mixed with 2.5 μg of expression plasmid, 5 μg of reporter plasmid, and 0.2 μg of SV-40 β-galactosidase plasmid. Transfection was performed by electroporation at 380 V and 950 mF (Gene Pulser XL; Bio-Rad) or using the Lipofectamine 2000 (Life Technologies) transfection reagent. Transfected cells were incubated in 60 mm culture dishes, for 24 h unless otherwise indicated, and fed with 10% fetal bovine serum and Dulbecco's modified Eagle's medium. Following lysis, assays for reporter activity (luciferase assay; Promega) as well as for protein concentration (Bradford assay; Bio-Rad) were carried out. β-galactosidase was measured using the Galacto-Light Plus reagents (Tropix, Inc) as an internal normalizer. For each assay, all luciferase activities were normalized to the mean value of the first experimental group and are shown as mean ± SEM.

EMSA

Complementary oligonucleotides containing a Lef-1-binding site within the *Dlx2* promoter with flanking partial

BamHI ends were annealed and filled with Klenow polymerase to generate ^{32}P-labeled probes for EMSAs as described (10). Standard binding assays were performed as previously described (10). A titration of the bacteria expressed and purified HMGN2 protein was used in the assays. Lef-1 purified protein was allowed to bind to the probe for 15 min, after which purified HMGN2 protein was titrated and added to the binding reaction. The samples were electrophoresed, visualized, and quantitated as described previously (10).

Western blot assays

Cell lysates were analyzed on 12% SDS-PAGE gels. Following electrophoresis, the protein was transferred to polyvinylidene difluoride membrane (Millipore), immunoblotted, and detected with a horseradish peroxidase–conjugated secondary Ab and ECL reagents from GE Healthcare/Amersham Biosciences. The following polyclonal Abs were used to detect the proteins: anti-β-tubulin (1:1000 dilution; Santa Cruz Biotechnology), anti-Pitx2 (1:500 dilution; Capra Science), and Hmgn2 (1:500 dilution; Millipore).

Real-time PCR assays

Total RNA was isolated from cells or mouse mandible and maxilla tissues using miRNeasy Mini Kit. Reverse transcription and quantitative real-time PCR were carried out with miScript PCR system (Qiagen) according to the manufacturer's protocol. All Ct numbers were below 35 cycles. PCR products were examined by melting curve analysis, and the sequences were confirmed. Fold changes were calculated using the $2^{-\Delta\Delta CT}$ method. The primers used for qPCR are listed in Table 1. The primers used to detect *miR-23a/b* were purchased from Qiagen.

Imaging and microcomputed tomography

Mouse heads of littermate WT and *HMGN2*$^{-/-}$ mice were dissected, fixed with 4% PFA overnight, and stored in 70% ethanol for imaging. Microcomputed tomography was conducted according to previous description (62).

ChIP assay

ChIP assays were performed as previously described (24) using the ChIP Assay Kit (Zymo Research). LS8 cells were crosslinked in 1% formaldehyde at room temperature for 7 min. Crosslinked cells were sonicated three times (6 s duration for each round, 25% of maximum amplitude) to shear the genomic DNA in to 200 to 1000 bp fragments. Then the DNA–protein complexes were immunoprecipitated with 5 μg Pitx2 Ab (Capra Science) or 5 μg rabbit IgG as control. Precipitated DNAs were subjected to PCR to evaluate the enrichment of Pitx2 binding.

The triple ChIP experiments were performed initially as described previously; however, after the initial IP with the chromatin factor and IgG control, the complexes were washed with high salt buffer to remove the Ab and resuspended in buffer. A second Ab and control IgG was used to pull down the complex again, and the isolated complexes were washed extensively in high salt buffer, followed by a third IP and reverse crosslinked and processed. The primers used for PCR are listed in Table 1. All the PCR products were analyzed on a 1.5% agarose gel for the correct size and confirmed by sequencing.

Co-IP assay

Lef-1-Hmgn2, Dlx2-Hmgn2, and FoxJ1-Hmgn2 endogenous complexes were IPed from LS-8 cells. Lef-1 Ab (Cell Signalling), Dlx2 Ab (Affinity BioReagents, Inc) and FoxJ1 Ab (Millipore) using 2 ug of Ab to pull down endogenous Hmgn2 using magnetic IgG Dynabeads (Thermo Fisher Scientific), then were washed and eluted according to the manufacturer's recommendations, and subjected to Western blot analysis. In other experiments, approximately 24 h after cell transfection with β-catenin, HMGN2, and Lef-1 (2.5 μg), CHO cells were rinsed with 1 ml of PBS and then incubated with 1 ml ice-cold radioimmunopreipitation assay buffer for 15 min at 4 °C. Cells were harvested and disrupted by repeated aspiration through a 25-gauge needle attached to a 1 ml syringe. The lysates were then incubated on ice for 30 min. Cellular debris was pelleted by centrifugation at 10,000*g* for 10 min at 4 °C. An aliquot of lysate was saved for analysis as input control. Supernatant was transferred to a fresh 1.5 ml microfuge tube on ice and precleared using the mouse ExactaCruz F IP matrix (ExactaCruz F; Santa Cruz Biotechnology) for 30 min at 4 °C. Matrix was removed by brief centrifugation, and supernatant was transferred to a new tube. An IP Ab–IP matrix complex was prepared as per the manufacturer's instructions using primary anti–β-catenin Ab (Millipore). The IP Ab–IP matrix complex was incubated with the precleared cell lysate at 4 °C for 12 h.

Table 1
The sequence of the mouse qPCR and ChIP primers used for this study

	Forward	Reverse
Genes and qPCR primers		
B-actin	GCCTTCCTTCTTGGGTATG	ACCACCAGACAGCACTGTG
Amelogenin	TACCACCTCATCCTGGAAGC	GTGATGAGGCTGAAGGGTGT
Pitx2	CTGGAAGCCACTTTCCAGAG	AAGCCATTCTTGCACAGCTC
Hmgn2	AAAACCAAGGTGAAGGACGA	TCTGTGCCTGGTCTGTTTTG
ChIP primers		
pre-*miR-23a*-27a-24-2 (Pitx2)	TCCTGCCCTAACCTGTCAGA	AGCTAAGGACCCAACCGACT
pre-*miR-23a*-27a-24-2 (con)	GCCTCCCTGTTTGATGTCTC	CAGCTGGTTCTGTCATGCTC.
pre-*miR-23b*-27b-24-1 (Pitx2)	GAGCTGAGACCTGCTCATCC	GGTGACTGACTGTCCTGTGC
pre-*miR-23b*-27b-24-1 (con)	TGTGTGTGTGTGATGTTTAAGGA	CAGCTTTCTTTCTGTGTCAATGAT

After incubation, the lysate was centrifuged to pellet the IP matrix. The matrix was washed two times with PBS and resuspended in 15 μl of double-distilled water and 3 μl 6× SDS loading dye. Samples were boiled for 5 min and resolved on a 10% polyacrylamide gel. Western blotting was used with anti-HMGN2 Ab and horseradish peroxidase–conjugated rabbit ExactaCruz F reagent to detect immunoprecipitated proteins.

Statistical analysis

All quantified results are presented as mean ± SEM and with an N value indicating the number of biological repeats. A two-tailed unpaired Student's t test and either one- or two-way ANOVA were used to determine statistical significance.

Data availability

All data are contained within the article.

Author contributions—B. H., M. B., and B. A. A. conceptualization; S. E., D. S., F. P., Z. S., Z. Z., X. L., M. S., and S. R. V. methodology; S. E. and B. A. A. formal analysis; S. E., D. S., F. P., Z. S., Z. Z., X. L., M. S., and S. R. V. validation; S. E., D. S., F. P., Z. S., Z. Z., X. L., M. S., and S. R. V. investigation; B. A. A. resources; B. H. and M. B. writing–review & editing; B. A. A. supervision; B. A. A. funding acquisition.

Abbreviations—The abbreviations used are: Ab, antibody; β-cat, β-catenin; BiFC, bimolecular fluorescence complementation; ChIP, chromatin immunoprecipitation; CHO, Chinese hamster ovary; CMV, cytomegalovirus; co-IP, coimmunoprecipitation; DSPP, dentin sialo phosphoprotein; EYFP, enhanced YFP; GST, gluta-thione-*S*-transferase; HEK-293, human embryonic kidney 293 cell line; HMGN2, high mobility group protein N2; IgG, immunoglob-ulin G; IP, immunoprecipitation; LaCL, labial cervical loop; MEF, mouse embryo fibroblast; miR, microRNA; PBST, PBS with Tween 20; PFS, paraformaldehyde; qPCR, quantitative PCR; TAC, transient amplifying cell; TG, transgenic; TSS, transcription start site.

References

1. Shirakawa, H., Herrera, J. E., Bustin, M., and Postnikov, Y. (2000) Targeting of high mobility group-14-17 proteins in chromatin is independent of DNA sequence. *J. Biol. Chem.* **275**, 37937–37944
2. Murphy, K. J., Cutter, A. R., Fang, H., Postnikov, Y. V., Bustin, M., and Hayes, J. J. (2017) HMGN1 and 2 remodel core and linker histone tail domains within chromatin. *Nucl. Acid Res.* **45**, 9917–9930
3. Garza-Manero, S., Sindi, A. A. A., Mohan, G., Rehbini, O., Jeantet, V. H. M., Bailo, M., *et al.* (2019) Maintenance of active chromatin states by HMGN2 is required for stem cell identity in a pluripotent stem cell model. *Epigenetics Chromatin* **12**, 73
4. Martínez de Paz, A., and Ausió, J. (2016) HMGNs: the enhancer charmers. *Bioessays* **38**, 226–231
5. He, B., Deng, T., Zhu, I., Furusawa, T., Zhang, S., Tang, W., *et al.* (2018) Binding of HMGN proteins to cell specific enhancers stabilizes cell identity. *Nat. Commun.* **9**, 5240
6. Bustin, M. (2001) Chromatin unfolding and activation by HMGN* chromosomal proteins. *Trends. Biochem. Sci.* **25**, 431–437
7. Trieschmann, L., Postnikov, Y. V., Rickers, A., and Bustin, M. (1995) Modular structure of chromosomal proteins HMG-14 and HMG-17; definition of a transcriptional activation domain distinct from the nucleosomal binding domain. *Mol. Cell. Biol.* **15**, 6663–6669
8. Catez, F., Yang, H., Tracey, K. J., Reeves, R., Misteli, T., and Bustin, M. (2004) Network of dynamic interactions between histone H1 and high-mobility-group proteins in chromatin. *Mol. Cell. Biol.* **24**, 4321–4328
9. Phair, R. D., and Mistell, T. (2000) High mobility of proteins in the mammalian cell nucleus. *Nature* **404**, 604–609
10. Amen, M., Espinoza, H. M., Cox, C., Liang, X., Wang, J., Link, T. M., *et al.* (2008) Chromatin-associated HMG-17 is a major regulator of homeo-domain transcription factor activity modulated by Wnt/beta-catenin signaling. *Nucl. Acids Res.* **36**, 462–476
11. Mohamed, O. A., Bustin, M., and Clarke, H. J. (2001) High-mobility group proteins 14 and 17 maintain the timing of early embryonic development in the mouse. *Dev. Biol.* **229**, 237–249
12. Lehtonen, S., Olkkonen, V. M., Stapleton, M., Zerial, M., and Lehto-nen, E. (1998) HMG-17, a chromosomal non-histone protein, shows developmental regulation during organogenesis. *Int. J. Dev. Biol.* **42**, 775–782
13. Travis, A., Amsterdam, A., Belanger, C., and Grosschedl, R. (1991) LEF-1, a gene encoding a lymphoid-specific protein with an HMG domain, regulates T-cell receptor a enhancer function. *Genes Dev.* **5**, 880–894
14. Amendt, B. A., Sutherland, L. B., Semina, E., and Russo, A. F. (1998) The molecular basis of rieger syndrome: analysis of Pitx2 homeodomain protein activities. *J. Biol. Chem.* **273**, 20066–20072
15. Semina, E. V., Reiter, R., Leysens, N. J., Alward, L. M., Small, K. W., Datson, N. A., *et al.* (1996) Cloning and characterization of a novel bicoid-related homeobox transcription factor gene, RIEG, involved in Rieger syndrome. *Nat. Genet.* **14**, 392–399
16. Gage, P. J., Suh, H., and Camper, S. A. (1999) The bicoid-related Pitx gene family in development. *Mamm. Genome* **10**, 197–200
17. Lin, C. R., Kioussi, C., O'Connell, S., Briata, P., Szeto, D., Liu, F., *et al.* (1999) Pitx2 regulates lung asymmetry, cardiac positioning and pituitary and tooth morphogenesis. *Nature* **401**, 279–282
18. Lu, M., Pressman, C., Dyer, R., Johnson, R. L., and Martin, J. F. (1999) Function of Rieger syndrome gene in left-right asymmetry and cranio-facial development. *Nature* **401**, 276–278
19. Wang, J., Saadi, I., Wang, J., Engel, J. J., Kaburas, A., Russo, A. F., *et al.* (2013) PIAS1 and PIASy differentially regulate PITX2 transcriptional activities. *J. Biol. Chem.* **288**, 12580–12595
20. Pispa, J., and Thesleff, I. (2003) Mechanisms of ectodermal organogenesis. *Dev. Biol.* **262**, 195–205
21. Tucker, A., and Sharpe, P. (2004) The cutting-edge of mammalian development; how the embryo makes teeth. *Nat. Rev. Genet.* **5**, 499–508
22. Vadlamudi, U., Espinoza, H. M., Ganga, M., Martin, D. M., Liu, X., Engelhardt, J. F., *et al.* (2005) PITX2, β-catenin, and LEF-1 interact to synergistically regulate the LEF-1 promoter. *J. Cell Sci.* **118**, 1129–1137
23. Amen, M., Liu, X., Vadlamudi, U., Elizondo, G., Diamond, E., Engelhardt, J. F., *et al.* (2007) PITX2 and β-catenin interactions regulate lef-1 isoform expression. *Mol. Cell. Biol.* **27**, 7560–7573
24. Sun, Z., Yu, W., Sanz Navarro, M., Sweat, M., Eliason, S., Sharp, T., *et al.* (2016) Sox2 and Lef-1 interact with Pitx2 to regulate incisor development and stem cell renewal. *Development* **143**, 4115–4126
25. Sweat, Y. Y., Sweat, M., Yu, W., Sanz-Navarro, M., Zhang, L., Sun, Z., *et al.* (2020) Sox2 controls periderm and rugae development to inhibit oral adhesions. *J. Dent. Res.* **99**, 1397–1405

26. van Genderen, C., Okamura, R. M., Farinas, I., Quo, R.-G., Parslow, T. G., Bruhn, L., *et al.* (1994) Development of several organs that require inductive epithelial-mesenchymal interactions is impared in LEF-1-deficient mice. *Genes Dev.* **8**, 2691–2703

27. Sasaki, T., Ito, Y., Xu, X., Han, J., Bringas, J.,P., Maeda, T., *et al.* (2005) LEF1 is a critical epithelial survival factor during tooth morphogenesis. *Dev. Biol.* **278**, 130–143

28. Zhao, Y., Ransom, J. F., Li, A., Vedantham, V., von Drehle, M., Muth, A. N., *et al.* (2007) Dysregulation of cardiogenesis, cardiac conduction, and cell cycle in mice lacking miRNA-1-2. *Cell* **129**, 303–317

29. Ucar, A., Vafaizadeh, V., Jarry, H., Fiedler, J., Klemmt, P. A. B., Thum, T., *et al.* (2010) miR-212 and miR-132 are required for epithelial stromal interactions necessary for mouse mammary gland development. *Nat. Genet.* **42**, 1101–1108

30. Grimson, A., Farh, K. K., Johnston, W. K., Garrett-Engele, P., Lim, L. P., and Bartel, D. P. (2007) MicroRNA targeting specificity in mammals: determinants beyond seed pairing. *Mol. Cell* **27**, 91–105

31. Cao, H., Wang, J., Li, X., Florez, S., Huang, Z., Venugopalan, S. R., *et al.* (2010) MicroRNAs play a critical role in tooth development. *J. Dent. Res.* **89**, 779–784

32. Shen, Y., Li, Y., Ye, F., Wang, F., Wan, X., Lu, W., *et al.* (2011) Identification of miR-23a as a novel microRNA normalizer for relative quantification in human uterine cervical tissues. *Exp. Mol. Med.* **43**, 358–366

33. Chen, Q., Xu, J., Li, L., Li, H., Mao, S., Zhang, F., *et al.* (2014) MicroRNA-23a/b and microRNA-27a/b suppress Apaf-1 protein and alleviate hypoxia-induced neuronal apoptosis. *Cell Death Dis.* **5**, e1132

34. Gao, P., Tchernyshyov, I., Chang, T. C., Lee, Y. S., Kita, K., Ochi, T., *et al.* (2009) c-Myc suppression of miR-23a/b enhances mitochondrial glutaminase expression and glutamine metabolism. *Nature* **458**, 762–765

35. Viswanathan, V., Damle, S., Zhang, T., Opdenaker, L., Modarai, S., Accerbi, M., *et al.* (2017) An miRNA expression signature for the human colonic stem cell niche distinguishes malignant from normal epithelia. *Cancer Res.* **77**, 3778–3790

36. Li, A., Song, T., Wang, F., Liu, D., Fan, Z., Zhang, C., *et al.* (2012) MicroRNAome and expression profile of developing tooth germ in miniature pigs. *PLoS One* **7**, e52256

37. Hu, C.-D., Chinenov, Y., and Kerppola, T. K. (2002) Visualization of interactions among bZIP and rel family proteins in living cells using bimolecular fluorescence complementation. *Mol. Cell* **9**, 789–798

38. Zhang, Z., Gutierrez, D., Li, X., Wang, J., Andrade, K., and Amendt, B. A. (2013) Homeodomain transcription factor Lhx6: a transcriptional repressor that interacts with PITX2 to regulate odontogenesis. *J. Biol. Chem.* **288**, 2485–2500

39. Li, X., Venugopalan, S., Cao, H., Pinho, F., Paine, M. L., Snead, M. L., *et al.* (2013) A model for the molecular underpinnings of tooth defects in axenfeld-rieger syndrome. *Hum. Mol. Genet.* **23**, 194–208

40. Cox, C. J., Espinoza, H. M., McWilliams, B., Chappell, K., Morton, L., Hjalt, T. A., *et al.* (2002) Differential regulation of gene expression by PITX2 isoforms. *J. Biol. Chem.* **277**, 25001–25010

41. Diamond, E., Amen, M., Hu, Q., Espinoza, H. M., and Amendt, B. A. (2006) Functional interactions between Dlx2 and lymphoid enhancer factor regulate Msx2. *Nucl. Acids Res.* **34**, 5951–5965

42. Green, P. D., Hjalt, T. A., Kirk, D. E., Sutherland, L. B., Thomas, B. L., Sharpe, P. T., *et al.* (2001) Antagonistic regulation of Dlx2 expression by PITX2 and Msx2: implications for tooth development. *Gene Expr.* **9**, 265–281

43. Espinoza, H. M., Cox, C. J., Semina, E. V., and Amendt, B. A. (2002) A molecular basis for differential developmental anomalies in Axenfeld-Rieger syndrome. *Hum. Mol. Genet.* **11**, 743–753

44. Venugopalan, S. R., Amen, M. A., Wang, J., Wong, L., Cavender, A. C., D'Souza, R. N., *et al.* (2008) Novel expression and transcriptional regulation of FoxJ1 during oro-facial morphogenesis. *Hum. Mol. Genet.* **17**, 3643–3654

45. Wibmuller, S., Kosian, T., Wolf, M., Finzsch, M., and Wegner, M. (2006) The high-mobility-group domain of Sox proteins interacts with DNA-binding domains of many transcription factors. *Nucl. Acids Res.* **34**, 1735–1744

46. Deng, T., Zhu, Z., Zhang, S., Postnikov, Y., Huang, D., Horsch, M., *et al.* (2015) Functional compensation among HMGN variants modulates the DNase I hypersensitive sites at enhancers. *Genome Res.* **25**, 1295–1308

47. Wang, Y., Li, X., and Hu, H. (2014) H3K4me2 reliably defines transcription factor binding regions in different cells. *Genomics* **103**, 222–228

48. Zhao, R., Nakamura, T., Fu, Y., Lazar, Z., and Spector, D. L. (2011) Gene bookmarking accelerates the kinetics of post-mitotic transcriptional reactivation. *Nat. Cell. Biol.* **13**, 1295–1304

49. Eliason, S., Sharp, T., Sweat, M., Sweat, Y. Y., and Amendt, B. A. (2020) Ectodermal organ development is regulated by a microRNA-26b-lef-1-Wnt signaling Axis. *Front. Physiol.* **11**, 780

50. Biehs, B., Hu, J. K., Strauli, N. B., Sangiorgi, E., Jung, H., Heber, R. P., *et al.* (2013) BMI1 represses Ink4a/Arf and Hox genes to regulate stem cells in the rodent incisor. *Nat. Cell Biol.* **15**, 846–852

51. Rochman, M., Postnikov, Y., Correll, S., Malicet, C., Wincovitch, S., Karpova, T. S., *et al.* (2009) The interaction of NSBP1/HMGN5 with nucleosomes in euchromatin counteracts linker histone-mediated chromatin compaction and modulates transcription. *Mol. Cell* **35**, 642–656

52. Rattner, B. P., Yusufzai, T., and Kadonaga, J. T. (2009) HMGN proteins act in opposition to ATP-dependent chromatin remodeling factors to restrict nucleosome mobility. *Mol Cell* **34**, 620–626

53. Fiorillo, A. A., Medler, T. R., Feeney, Y. B., Liu, Y., Tommerdahl, K. L., and Clevenger, C. V. (2011) HMGN2 inducibly binds a novel transactivation domain in nuclear PRLr to coordinate Stat5a-mediated transcription. *Mol. Endocrinol.* **25**, 1550–1564

54. Furusawa, T., Lim, J.-H., Catez, F., Birger, Y., Mackem, S., and Bustin, M. (2006) Down-regulation of nucleosomal binding protein HMGN1 expression during embryogenesis modulates *Sox9* expression in chondrocytes. *Mol. Cell. Biol.* **26**, 592–604

55. Zhu, X., Gleiberman, A. S., and Rosenfeld, M. G. (2007) Molecular physiology of pituitary development: signaling and transcriptional networks. *Physiol. Rev.* **87**, 933–963

56. Hock, R., Furusawa, T., Ueda, T., and Bustin, M. (2007) HMG chromosomal proteins in development and disease. *Trends Cell Biol.* **17**, 72–79

57. Venugopalan, S. R., Li, X., Amen, M. A., Florez, S., Gutierrez, D., Cao, H., *et al.* (2011) Hierarchical interactions of homeodomain and forkhead transcription factors in regulating odontogenic gene expression. *J. Biol. Chem.* **286**, 21372–21383

58. Lehtonen, S., and Lehtonen, E. (2001) HMG-17 is an early marker of inductive interactions in the developing mouse kidney. *Differentiation* **67**, 154–163

59. Bustin, M., and Neihart, N. K. (1979) Antibodies against chromosomal HMG proteins stain the cytoplasm of mammalian cells. *Cell* **16**, 181–189

60. Lim, J.-H., West, K. L., Rubinstein, Y., Bergel, M., Postnikov, Y. V., and Bustin, M. (2005) Chromosomal protein HMGN1 enhances the acetylation of lysine 14 in histone H3. *EMBO J.* **24**, 3038–3048

61. Chen, L. S., Couwenhoven, R. I., Hsu, D., Luo, W., and Snead, M. L. (1992) Maintenance of amelogenin gene expression by transformed epithelial cells of mouse enamel organ. *Arch. Oral Biol.* **37**, 771–778

62. Sun, Z., da Fontoura, C. S. G., Moreno, M., Holton, N. E., Sweat, M., Sweat, Y., *et al.* (2018) FoxO6 regulates Hippo signaling and growth of the craniofacial complex. *PLoS Genet.* **14**, e1007675

ASBMB